8-2011

Discharge Coefficients of Oblique Weirs

Samuel Egnew Tingey
Utah State University

DISCHARGE CHARACTERISTICS OF OBLIQUE WEIRS

by

Samuel Egnew Tingey

A thesis submitted in partial fulfillment
of the requirements for the degree

of

MASTER OF SCIENCE

in

Mechanical Engineering

Approved:

_____	_____
Barton Smith Major professor	Blake P. Tullis Committee Member
_____	_____
Robert E. Spall Committee Member	Dr. Mark R. McLellan Vice President for Research and Dean of the School of Graduate Studies

UTAH STATE UNIVERSITY
Logan, Utah

2011

ABSTRACT

Discharge Coefficients of Oblique Weirs

by

Samuel Egnew Tingey, Master of Science

Utah State University, 2011

Major Professor: Dr. Barton Smith
Department: Mechanical and Aerospace Engineering

Oblique weirs are those weirs placed at an angle with respect to the channel centerline. They can be used in canal applications where more discharge is needed, but there is limited freeboard. The discharge coefficients were determined for 54 different weirs by measuring total head for various flows over each weir. These weirs included sharp, half round and quarter-round-crested weirs. There were 18 weirs for each crest shape with three weir heights for each angle tested. The oblique angles tested were 10°, 15°, 25°, 45°, 60°, and 90° with respect to the channel centerline, with the nominal weir heights being 4, 8, and 12 inches. The half-round-crested weirs were the most efficient, followed by the quarter-round-crested weirs and the sharp-crested weirs were the least efficient. By decreasing the oblique angle, the weir length became longer and the weir would be more efficient than the normal weir.

(62 pages)

ACKNOWLEDGMENTS

I would like to thank many people for their help on this project. I would like to thank Dr. Blake Tullis for his unending patience with a mechanical engineer working at the UWRL. I would like to thank Dr. Barton Smith for being so flexible and supportive. I would like to acknowledge Brian Crookston and Ricky Anderson for their help and encouragement. All the guys in the UWRL shop were extremely helpful. Finally, I would like to tell my wife, Laura, and son, Andrew, that I love them and thank them for their love and support.

Sam Tingey

CONTENTS

Page

LIST OF TABLES

LIST OF FIGURES

LIST OF SYMBOLS

The following symbols were used in this thesis:

A = cross-sectional flow area

A_t = orifice throat area

C_c = contraction coefficient

C_d = dimensionless weir discharge coefficient based on effective weir length and total upstream head

C_{dH} = dimensionless weir discharge coefficient based on full centerline weir length and upstream piezometric head

C_{dw} = dimensionless weir discharge coefficient determined by Noori and Chilmeran

C_o = dimensionless orifice discharge coefficient

D_p = inside pipe diameter

D_t = orifice throat diameter

g = acceleration due to gravity

H = upstream piezometric head

H_t = total upstream head

H = position above the top of the weir crest

K = parameter for Borghei et al head discharge relationships

L = full centerline weir length

L_e = effective weir length

P = weir height

Q = water volumetric flow rate

q = discharge per unit length of oblique weir

q_n = discharge per unit length of normal weir

R = radius of curvature for rounded topped weirs

t = weir thickness

V = average water velocity

W = width of channel

W_c = width of one cycle of a labyrinth weir

X = reading of digital multimeter in mA

α = angle of weir measured from channel centerline

β = ratio of diameters for the orifice discharge equation

β_A = Parameter in Aichel relationship

ΔH = differential head

Ω = uncertainty

INTRODUCTION

Weir structures are dam-like structures used in canal, river, and reservoir applications for flow measurement, flow diversion, and/or discharge control. They are typically designed for free-flow conditions and are positioned normal to the direction of flow. A normal linear weir is commonly used in canal applications as a diversion structure, which is a structure that raises the water level upstream of the weir sufficiently to permit water diversion into another canal or pipeline.

In canal applications where diversion is required but the freeboard, the distance between the water level and where flooding would occur, is limited, a normal linear weir may not have the capacity to pass the required flood discharge with the limited freeboard available. Increasing weir length is one way to increase discharge capacity without raising the total upstream head. Widening the canal to allow for a longer normal weir is impractical for most applications; however, using a longer linear weir installed at an angle $\alpha < 90°$ to channel centerline (oblique weir), as shown in Fig. 1, is a plausible

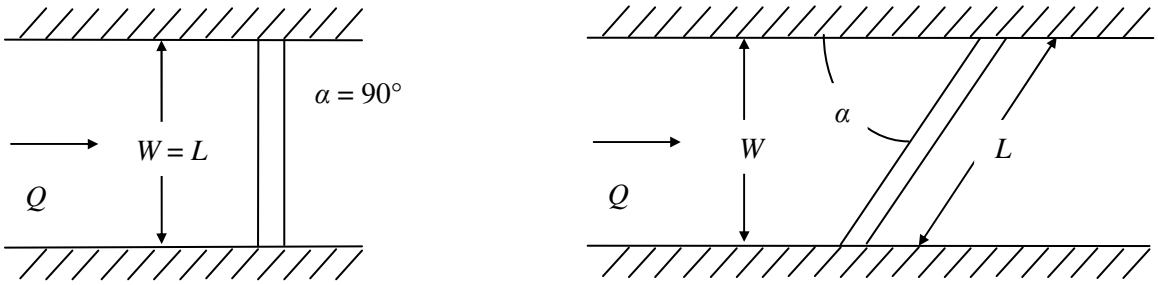

(a) (b)

Figure 1. Plan view of (a) normal weir and (b) oblique weir.

solution. In addition to increasing the weir length, the weir head-discharge relationship may also be influenced by the weir crest shape. A crest with a rounded upstream edge (quarter round) could be more efficient (higher Q for a given H) than the sharp-crested weir; a crest rounded on both the upstream and downstream sides (half round) could be more efficient than either the sharp-crested or quarter round shapes (see Fig 2).

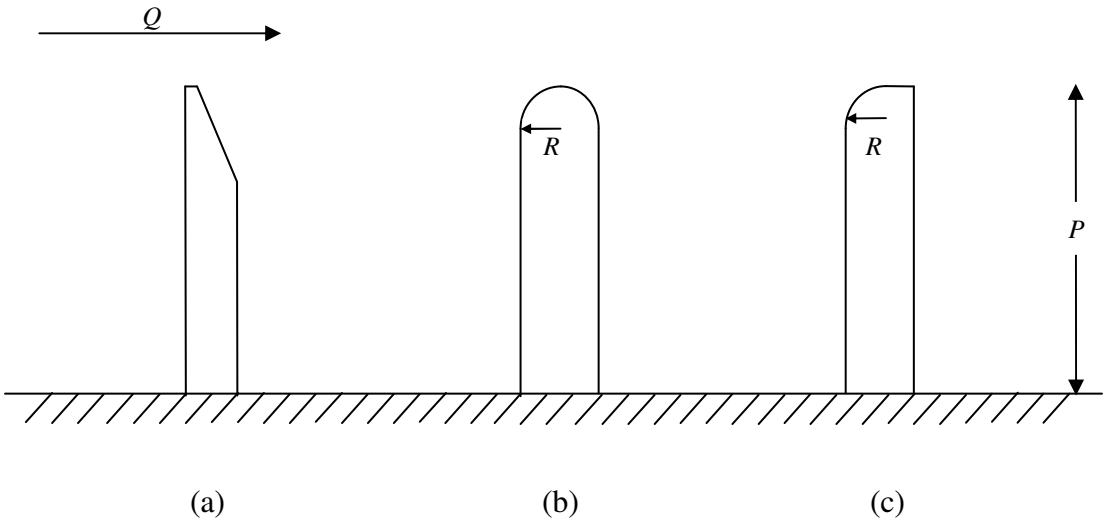

Figure 2. Different crest shapes: (a) sharp, (b) half round, and (c) quarter round.

LITERATURE REVIEW

Weir Equation

Henderson [1] explains that starting with a sharp-crested weir placed normally in a channel, the flow will be substantially free from viscous effects because opportunities for boundary-layer development are limited to the vertical face of the weir where velocities are low. Also, with the weir crest running the full width of the channel, the flow is essentially two-dimensional because the channel sidewalls suppress the lateral contraction effects. Figure 3 shows the longitudinal section of flow over such a weir. Assuming the flow does not contract as it passes over the weir as shown in Fig. 3(a), and that the pressure is atmospheric everywhere between the top of the weir and the water level, an elementary analysis can be made. Under these assumptions, the velocity at any point is equal to $\sqrt{2gh}$ where the depth h is measured down from the total energy line. The discharge per unit width q is given by Eq. (1) as

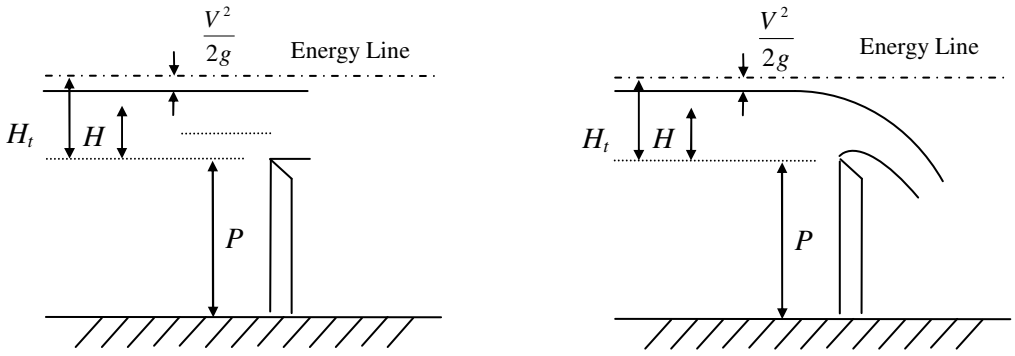

(a) (b)

Figure 3. Sharp-crested weir (a) without flow contraction and (b) with flow contraction.

$$q = \int_{V^2/2g}^{H_t} \sqrt{2gh}\,dh = \frac{2}{3}\sqrt{2g}\left[H_t^{3/2} - \left(\frac{V^2}{2g}\right)^{3/2} \right] \quad (1)$$

The effect of the flow contraction, as shown in Fig. 3(b), may be expressed by a contraction coefficient C_c, resulting in

$$q = \frac{2}{3} C_c \sqrt{2g}\left[H_t^{3/2} - \left(\frac{V^2}{2g}\right)^{3/2} \right] \quad (2)$$

This can be compacted by introducing a discharge coefficient C_d making Eq. (2) become

$$q = C_d \frac{2}{3}\sqrt{2g} H_t^{3/2} \quad (3)$$

where

$$C_d = C_c\left[1 - \left(\frac{V^2}{2gH_t}\right)^{3/2} \right] \quad (4)$$

Finally, by multiplying Eq. (3) by the weir length, the standard weir equation is shown as

$$Q = C_d \frac{2}{3}\sqrt{2g} L H_t^{3/2} \quad (5)$$

The effects from placing the weir at an oblique angle should be taken into C_d.

Oblique Weirs

Though normal weirs have been studied extensively, only limited information regarding the hydraulic characteristics of oblique weirs is available in the literature. One of the first studies of oblique weirs was performed by Aichel [2] who developed a relationship between the discharges for normal and oblique weirs at different angles as

$$\frac{q}{q_n} = 1 - \frac{H}{P}\beta_A \tag{6}$$

where q is the discharge per unit length of the oblique weir, q_n is the discharge per unit width of the normal weir, and β is a coefficient dependent α (i.e. β_A increases exponentially as α decreases).

Borghei et al. [3] experimentally determined C_{dH} for oblique sharp-crested weirs over a small range of *H/P,* about 0.08 to about 0.21. In this range, they found linear relationships between C_{dH} and *H/P* for seven different oblique angles, α = 26°to 61°, which are shown in Fig. 4. Equation (7) is a general relationship of C_{dH} vs *H/P* developed by Borghei et al. [3], where the effects of α are characterized by *W/L* (channel width over weir length).

$$C_{dH} = \left(0.701 - 0.121\frac{W}{L}\right) + \left(2.229\frac{W}{L} - 1.663\right)\frac{H}{P} \tag{7}$$

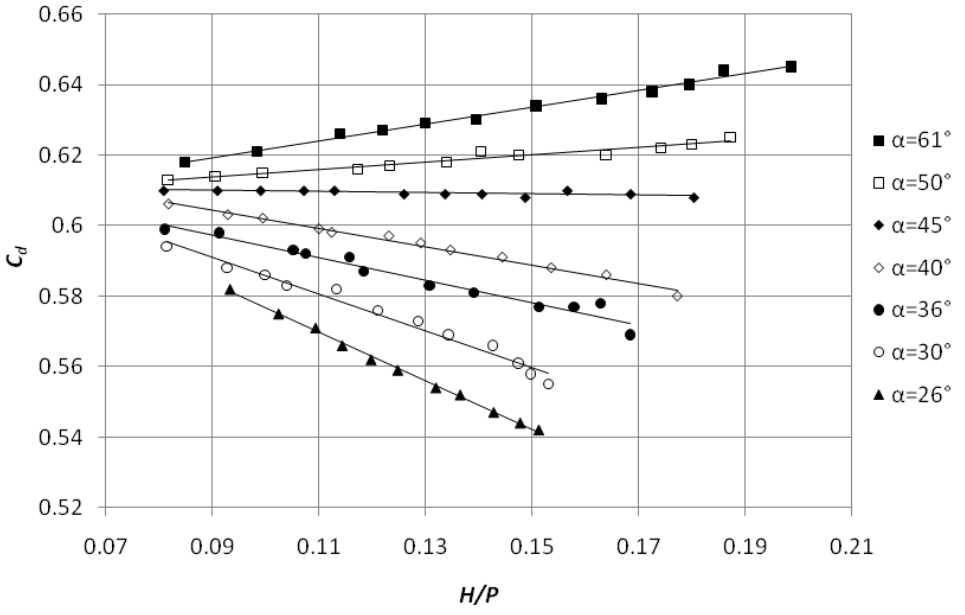

Figure 4. C_d plotted against *H/P* for different α based on Borghei et al. [3].

downstream water head over the weir. Borghei et al. [4] used the data from Borghei et al. [3] and using incomplete self-similarity, developed four *H-Q* equations to describe the flow characteristics of oblique sharp-crested weirs. Borghei et al. [4] show that Eq. (8)-Eq. (11) have better agreement with the data from Borghei et al. [3] than Eq. (3).

$$\frac{H}{P} = 1.005 \exp\left[0.277\left(\frac{L}{W}\right)\right]\left(\frac{K}{P}\right) \tag{8}$$

$$\frac{H}{P} = 0.982 * 10^{0.129(L/W)}\left(\frac{K}{P}\right)^{0.89\exp[0.09(L/W)]} \tag{9}$$

$$\frac{H}{P} = 1.34 * 10^{0.03(L/W)}\left(\frac{K}{P}\right)^{1.007} \tag{10}$$

$$\frac{H}{P} = \left[1.068 + 0.292\left(\frac{L}{W}\right)\right]\left(\frac{K}{P}\right)^{0.939+0.048(L/W)} \tag{11}$$

where

$$K = \left(\frac{Q}{\sqrt{g}L}\right)^{2/3} \tag{12}$$

These equations provide only a modest improvement in accuracy and are more difficult to use relative to Eq. (7). The main advantage according to Borghei et al. [4] is Eq (8) through Eq. (11) have over Eq. (7) is that they include the 90° weir where Eq. (7) does not. Data from the current study will be compared with Eq. (7).

Borghei et al. [3] and Borghei et al. [4] limited their experimental data to relatively small *H/P* values where velocity heads are minor. Extrapolating their empirical results to higher *H/P* values, where the velocity head may be significant, may be problematic as approach flow velocity will likely influence the weir head-discharge

relationship. The total upstream head is likely a more appropriate representation of the upstream driving head; the range of H/P (or H_t/P) should be expanded to develop a more complete understanding of oblique weir hydraulics.

Noori and Chilmeran [5] experimentally determined a different discharge coefficient C_{dw} for normal and oblique weirs with half round crests that varied in R of 5 cm, 7.5 cm and 10 cm; for P of 20 cm, 25 cm, 30 cm; and 35 cm; and for α of 30°, 45°,60°, and 90°, measured relative to the channel centerline. They developed the following relationship between C_{dw}, H/P, R/P, and α.

$$C_{dw} = \frac{0.674}{(H/P)^{0.15}(R/P)^{0.54}(\sin\alpha)^{0.86}} \tag{13}$$

To make C_{dw} comparable to C_d, the following operation can be performed

$$C_d = \frac{W}{L}\frac{3}{2\sqrt{2g}}C_{dw} \tag{14}$$

Noori and Chilmeran found that for an oblique half-round-crested weir with a given R, the discharge coefficient varies with P, as shown in Fig. 5. The general applicability of Eq. (13) may be somewhat limited due to the use of H rather than H_t. With the correlation coefficient for Eq. (13), relative to the data in Fig. 5, being relatively low (0.85), Eq. (13) was going to be evaluated using the data set developed in the current study until it was found that Eq. (13) could not be independently verified using the Noori and Chilmeran [5] data from which it was developed. Results from Eq. (13) did not match the data given by Noori and Chilmeran.

Other studies on oblique weirs include De Vries [6] who experimentally determined C_d for normal and oblique trapezoidal or dike form weirs with α = 30°, 45°,

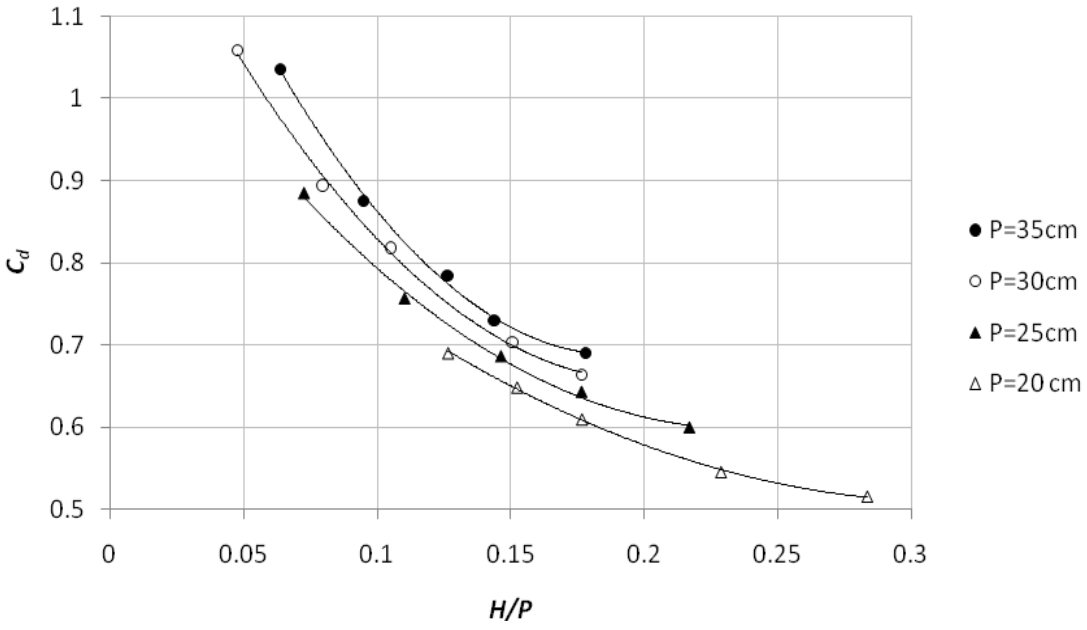

Figure 5. C_d plotted against H/P for $\alpha = 30°$, $R = 5$ cm with different P based on Noori and Chilmeran [5].

60°. These C_d values were compared by Wols et al. [7] and Uijttewaal [8] to numerical model results of the submerged oblique trapezoidal weir. They found good correlation between De Vries' data and their numerical model. Wols et al. developed the model and Uijttewaal furthered the research to include submerged objects that act as oblique weirs. Tuyen [9] experimentally determined C_d for an oblique trapezoidal weir as well. He also determined C_d for oblique sharp-crested and broad crested weirs set at $\alpha = 45°$ and the resulting C_d data compared well with that of Borghei et al. [3] and De Vries [6].

No literature could be found on oblique quarter-round-crested weirs. There have been studies conducted on labyrinth weirs with quarter round crests. These studies may be useful in understanding the discharge characteristics of oblique quarter-round-crested weirs.

Labyrinth Weirs

Labyrinth weirs are linear weirs that have been folded in plan view, with a crest profile that may be rectangular, trapezoidal or triangular. Figure 6 shows one cycle examples of each labyrinth weir type. The non-rectangular labyrinth weir geometries are effectively sequences of oblique weirs.

Tullis et al. [10] experimentally measured C_d for trapezoidal labyrinth weirs with quarter round crests and developed a relation between C_d and H_t/P for $\alpha = 6°$ to 35°. Figure 7 shows C_d determined by Tullis et al. for a trapezoidal labyrinth weir with quarter round crest. The data for the trapezoidal labyrinth weir with a quarter round crest with $\alpha = 8°$ were corrected by Willmore [11]. A curve for a 10° labyrinth weir can be interpolated between Tullis el al. 12° data and Willmore 8° data. This can be compared with the oblique 10° quarter round crest data. Comparisons can also be made between the 15° and 25° labyrinth and oblique weirs with quarter round crests.

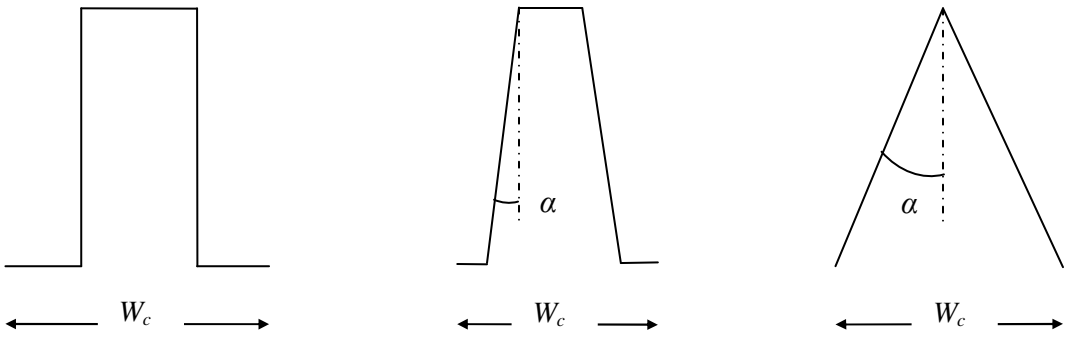

Figure 6. Labyrinth weirs: (a) rectangular, (b) trapezoidal, and (c) triangular.

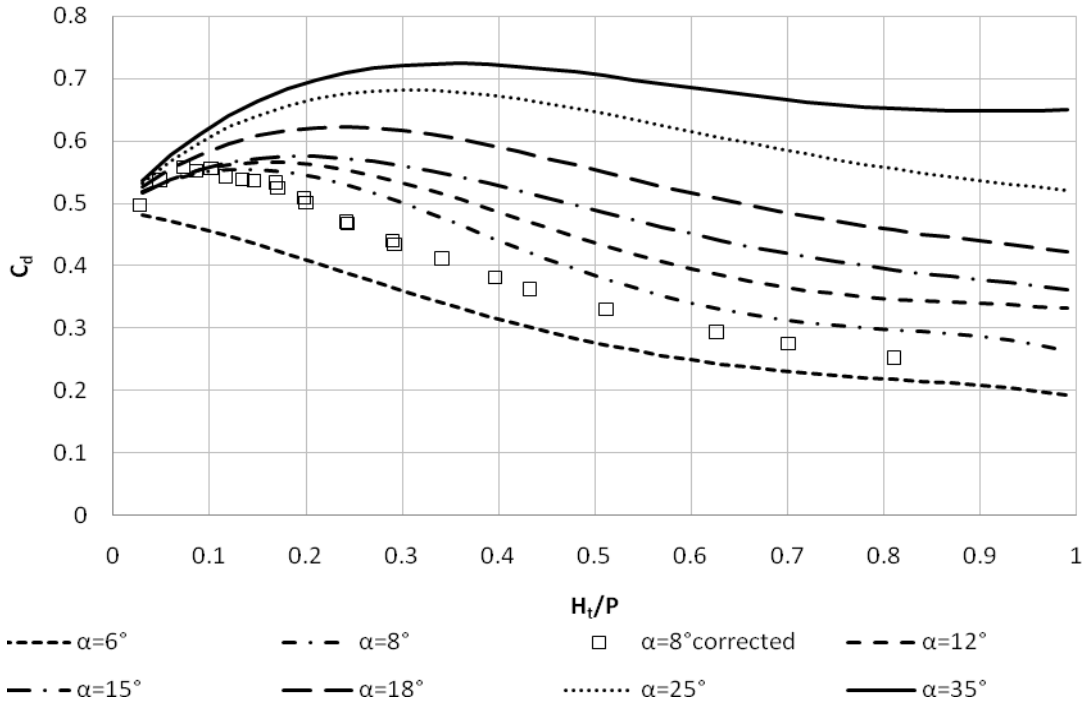

Figure 7. C_d plotted against H_t/P for trapezoidal labyrinth weirs of different α based on Tullis et al. [10] and Willmore [11].

Willmore also experimentally measured C_d for trapezoidal labyrinth weirs with half round crests. He built two-cycle trapezoidal labyrinth weirs with α = 7°, 8°, 10°, 12°, 15°, 20°, and 35°. A curve for a 25° labyrinth can be interpolated to be compared with the 25° oblique half round crest weir. Comparisons can also be made between the 10° and 15° labyrinth and oblique weirs.

The presence of labyrinth weir apexes can decrease the discharge capacity, due to the fact that some of the weir length becomes less or ineffective (e.g. apex corners). Tullis et al. introduce the idea of replacing the total weir length, L, in the weir equation, Eq. (5), with an effective length L_e when calculating Q and C_d. The effective length removes the weir length associated with the apex of the labyrinth weir as shown in Fig. 8.

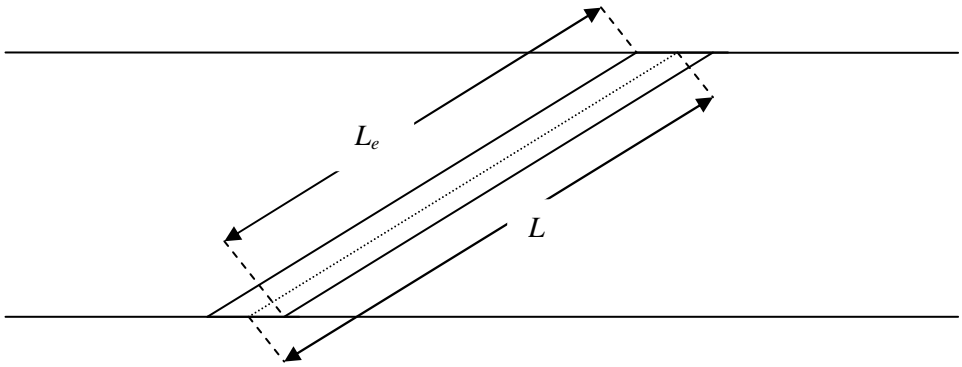

Figure 8. The effective length L_e is different from the weir centerline length L.

Even though oblique weirs typically do not feature labyrinth weir-type apexes, they have been observed (current study) to have similar ineffective weir regions where the weir meets the channel wall.

Objectives

To better understand the effect that an oblique angle has on the discharge coefficient of a weir, the following research objectives were investigated in this study.

1. Construct oblique weirs with variable crest shape and height. The crest shapes of interest will include sharp-crested, half round, and quarter round. The differing heights will allow for a wider range of H_t/P.
2. Measure head-discharge data for each crest with α = 10°, 15°, 25°, 45°, 60°, and 90° over a wide range of free flow discharges. A total of 54 weirs will be tested. Calculate C_d for each weir configuration and flow condition.
3. Compare calculated C_d values with those given by others who have studied oblique weirs and labyrinth weirs previously.

4. Develop efficiency curves by plotting C_d versus H_t/P for the three different crest shapes and six angles to be used for oblique weir design. Demonstrate how discharge efficiency varies with α and crest shape.

EXPERIMENT SETUP AND PROCEDURE

Flume Description

All testing was conducted at the Utah Water Research Laboratory (UWRL) at Utah State University in a level rectangular horizontal flume that was 24 feet long, 2 feet wide, and 2 feet deep. The flume had a 12-inch diameter supply line with a flow capacity of approximately 8.5 cubic feet per second (cfs). The bottom of the flume was painted steel and the sidewalls were clear acrylic for viewing. An adjustable platform was placed on the floor of the flume for leveling the weir. A flow straightener made of wooden slats and wire mesh was placed in the flume to create uniform approach flow. The upstream water depth, measured relative to the crest elevation, was determined using a stilling well mounted to a wall equipped with a point gage hydraulically connected via a pressure tap mounted in the flume wall 3 feet upstream from the upstream corner of the weir. The stilling well was a cylindrical tube that is 5 inches in diameter. In the stilling well, the water surface was calmed so waves and fluctuations would not interfere with the measurement of H. The upstream velocity head was calculated at that location by dividing Q by the cross sectional flow area. A sketch of the flume is shown in Fig. 9.

Weir Description

The weir was constructed of 1-inch thick high-density polyethylene (HDPE) sheeting material. The weir was constructed with four stackable pieces to allow for height adjustment, including a 2-inch tall base, two 4-inch tall removable middle pieces, and a 2-inch tall crest piece for each of the crests tested. The crest shapes were sharp-

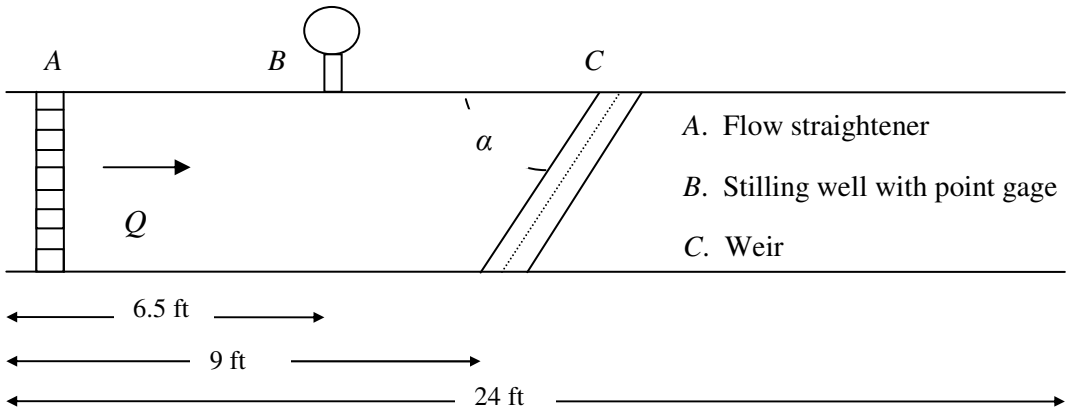

Figure 9. Plan sketch of experimental setup (not to scale).

crested, half round and quarter round crests. Steel inserts were placed in between the weir sections, creating a spline joint assembly, to provide stability and leak protection. The upstream horizontal joints of the modular weir walls were sealed with clear packaging tape. The bottom of the weir was sealed with a caulking material (NP1); the sides were sealed with plumber's putty to facilitate weir height changes. The 10° oblique weir was built first and after collecting data for all heights and crest shapes, the weir was cut to the appropriate length for the next angle. A summary of the tested weir geometries is given in Table 1.

Point Gages

Two precision point gages were used to determine the elevation of the weir crest and to obtain the water surface elevations of the approaching flow. The gages had vernier scales marked in 0.001 feet divisions. One point gage was placed in the stilling well to measure *H* and the other was used to help determine the weir crest elevation. The second point gage was placed over the weir and by filling the flume with water to just

Table 1. Weir Geometry for Each Experimental Setup

α (°)	L (inch)	L_e (inch)	P (inch)		
			Sharp-crested	Half round	Quarter round
10	138.2	127	11.196 7.236 3.240	11.232 7.260 3.252	11.232 7.248 3.240
15	92.7	85.3	11.256 7.320 3.264	11.232 7.272 3.300	11.256 7.236 3.240
25	56.8	52.5	11.256 7.320 3.240	11.268 7.260 3.276	11.244 7.248 3.240
45	33.9	31.9	11.088 7.020 3.108	11.088 7.056 3.084	11.076 7.032 3.096
60	27.7	26.6	11.160 7.164 3.204	11.160 7.212 3.204	11.160 7.032 3.204
90	23.8	23.8	11.184 7.212 3.060	11.184 7.188 3.060	11.196 7.032 3.060

below the weir crest; a difference between the weir crest and the water surface could be measured and added to the point gage in the stilling well to determine the crest elevation reference. Knowing the crest elevation reference, it is possible to measure H on the weir.

The second point gage also was used to determine P for each weir because of variations in installation. After leveling the weir, the point gage was used to measure the elevation difference between the weir crest and the leveling platform (P). The weir height was measured at five different locations; the average P value was assumed to be representative of the weir height.

Flow Measurement

The flow through the flume was measured using two circular orifice plates with

inner diameters of 10.297 inches and 7.044 inches. Both orifice plates were calibrated with a weigh tank, traceable to the National Institute of Standards and Technology (NIST). The 10.297-inch orifice plate was used for the 10° oblique weir and the 7.044-inch orifice plate was used for all the other weirs. Pressure taps were located at 1 pipe diameter upstream (1 foot) and a 1/2 pipe diameter downstream (0.5 feet) of the orifice plate. The pressure taps were connected to Rosemount differential pressure transmitters. For low flows, the pressure taps were connected to a differential pressure transmitter with a range of 25 inches of water and for high flows they were connected to one with a range of 1000 inches of water. Each could be spanned to 10% of its range making them useful for ranges between 2.5-100 inches of water, which were needed for the flows encountered in the experiments. The differential pressure transmitters were connected to a digital multimeter to get a reading X in milliamps (mA), with X =4 mA being the no flow condition. This reading was converted into a differential head ΔH in feet using Eq. (15).

$$\Delta H = \frac{(X-4)}{16}\frac{Range}{12} \tag{15}$$

Q, in cfs, was calculated using ΔH in the head-discharge equation for an orifice, Eq. (16).

$$Q = C_O A_t \sqrt{\frac{2g\Delta H}{1-\beta^4}} \tag{16}$$

with

$$\beta = \frac{D_t}{D_p} \tag{17}$$

where C_o is the discharge coefficient of the orifice plate, A_t is the area of the orifice throat, D_t is the orifice throat diameter, and D_p is the pipe diameter.

Calculations

An Excel spreadsheet was used to calculate Q, H_t, and C_d. The C_d vs H_t data were plotted for immediate analysis of data as it was recorded. Equations (15) through (21) were used to make the calculations in this spreadsheet. The variables in Eq. (18) through Eq. (21) were determined at the location of the tap leading to the stilling well.

$$A = (P + H)W \tag{18}$$

$$V = \frac{Q}{A} \tag{19}$$

$$H_t = H + \frac{V^2}{2g} \tag{20}$$

$$C_d = \frac{Q}{\frac{2}{3}\sqrt{2g}\,L_e H_t^{3/2}} \tag{21}$$

where V is the average approach velocity of the water.

Uncertainty

The variables with uncertainty ω in the experiment are Q, L_e, P, W, and H. The uncertainties are:

$$\omega_Q = \pm 0.25\%$$

$$\omega_{Le} = \pm 1/32 \text{ in}$$

$$\omega_P = \pm 0.0005 \text{ ft}$$

$$\omega_W = \pm 1/32 \text{ in}$$

$$\omega_H = \pm 0.0005 \text{ ft}$$

The uncertainty in the measurements was determined following an approach

given by Kline and McClintock [12] for single-sample experiments. To assess the uncertainty of C_d, Eq. (21) should be differentiated with respect to each variable where uncertainty exists and then multiplied the amount of uncertainty for that variable. These results are squared, summed, and finally the square root is taken. This value is divided by C_d to determine the ratio of the error of C_d for the given conditions. This is shown in Eq. (22) through Eq. (25).

$$\omega_{Cd} = \frac{\left[\left(\frac{\partial C_d}{\partial Q}\omega_Q\right)^2 + \left(\frac{\partial C_d}{\partial L_e}\omega_{L_e}\right)^2 + \left(\frac{\partial C_d}{\partial P}\omega_P\right)^2 + \left(\frac{\partial C_d}{\partial H_t}\omega_{H_t}\right)^2\right]^{0.5}}{C_d} \tag{22}$$

where

$$\omega_{H_t} = \frac{\left[\left(\frac{\partial H_t}{\partial H}\omega_H\right)^2 + \left(\frac{\partial H_t}{\partial V}\omega_V\right)^2\right]^{0.5}}{H_t} \tag{23}$$

where

$$\omega_V = \frac{\left[\left(\frac{\partial V}{\partial Q}\omega_Q\right)^2 + \left(\frac{\partial V}{\partial A}\omega_A\right)^2\right]^{0.5}}{V} \tag{24}$$

where

$$\omega_A = \frac{\left[\left(\frac{\partial A}{\partial P}\omega_P\right)^2 + \left(\frac{\partial A}{\partial H}\omega_H\right)^2 + \left(\frac{\partial A}{\partial W}\omega_W\right)^2\right]^{0.5}}{A} \tag{25}$$

The results of this analysis show that the largest uncertainty in C_d from Eq. (22) is for the weirs with smallest P, longest L_e, and lowest H_t. The maximum uncertainty is 1.05%. All other uncertainties are below 1.0%.

Approach Condition

The upstream apex (i.e. joint between the weir and the flume sidewall) of the oblique weir was located 8 feet downstream of the flume inlet to accommodate the length of the 10° oblique weir. As the weir was shortened for each α, the upstream apex of the weir was kept in the same position. To evaluate the relatively short approach flow section, sharp-crested normal weir, located at both the upstream apex and the downstream at the end of the flume was tested. Figure 10 shows that the agreement C_d data from both experiments are in good agreement with each other (1.5% or better). The data also compare relatively well (3% or better) with the normal sharp-crested weir data reported by Johnson [12], suggesting that the short approach flow length had minimal influence on the experimental results.

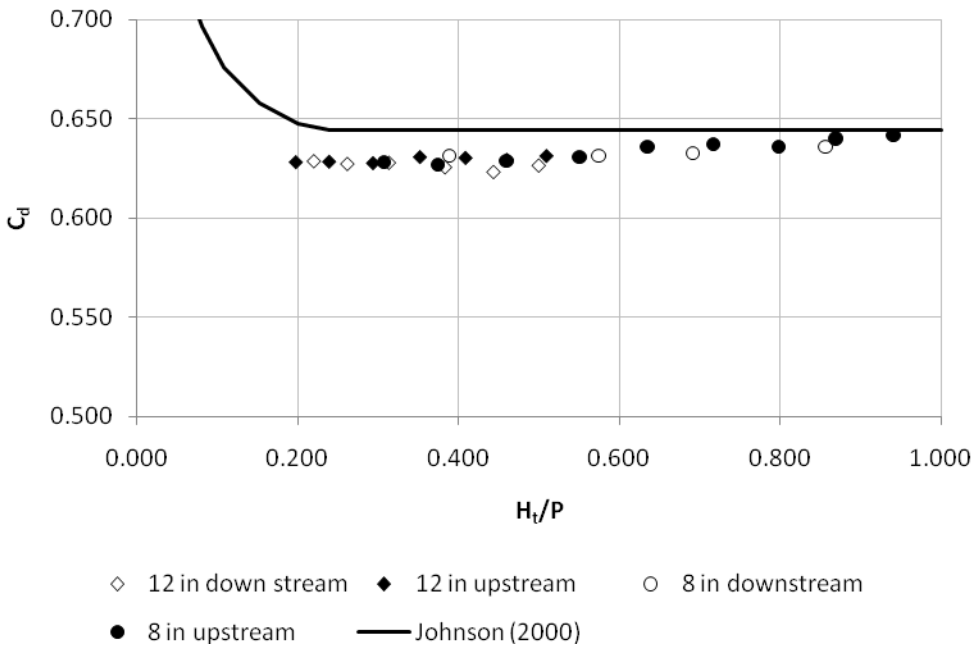

Figure 10. Comparison of C_d values for different locations of aerated normal sharp crested weir and comparison to results of Johnson [12].

Nappe

The nappe refers to the jet of water passing over the weir as shown in Fig. 11. Nappe aeration conditions affect C_d. The nappe can be aerated or non-aerated and the aerated nappe can be vented or non-vented. With a non-aerated nappe, the water clings to the downstream side of the weir and no air gets behind the nappe. The nappe is held against the weir by negative pressure that on the downstream side of the weir. The negative pressure also increases C_d making the weir more efficient. A non-aerated or clinging nappe condition occurred at low values of H_t/P or when weir-submerging (tailwater elevation exceeds the weir crest elevation) or near submerging tailwater conditions exist. When the momentum of the nappe is sufficiently large to cause it to detach or separate from the downstream face of the weir, an air pocket form, with entrained air serving as the air source. A vented, aerated nappe refers to a condition where an air vent is provided, supplying air to the underside of the nappe at atmospheric

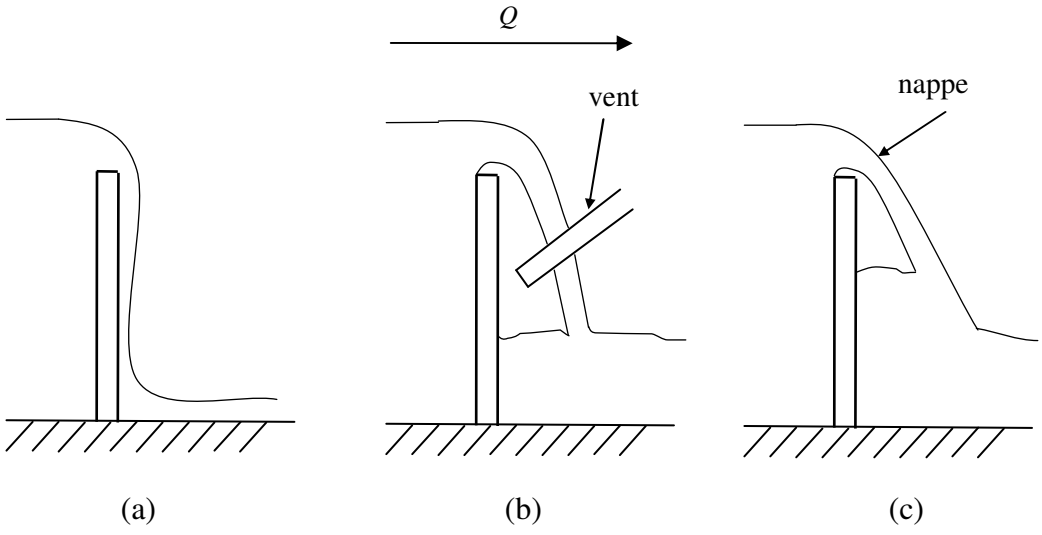

Figure 11. Different nappe conditions: (a) Non-aerated, (b) Aerated vented, and (c) aerated non-vented.

pressure. Without the aid of the negative pressure, C_d can be lower than non-vented nappe condition. The sub-atmospheric pressure associated with the vented, non-aerated nappe causes the water level behind the nappe to be at a higher level than the tail water downstream. For experimental oblique weirs with small values of α, an aerated, vented nappe condition was typically present due to the presence of a naturally occurring air vent that developed at the downstream weir apex resulting from flow separation.

Another important nappe condition is stability. An unstable nappe is one where the pressure under the nappe fluctuates. The fluctuations from an unstable nappe result in fluctuating force loads on the structure. A stable nappe for normal weirs is typically maintained by having a vented condition where the constant atmospheric pressure does not allow for fluctuations to occur. With oblique weirs, nappe venting may not be adequate to maintain a stable nappe condition for all flow conditions due to the tailwater influences just discussed.

EXPERIMENTAL RESULTS

Flow Regimes

The aerated nappe condition was segregated by Johnson [12] into two different flow regimes, leaping flow, where the nappe detaches from the downstream side of the crest, and springing flow, where the nappe detaches farther up on the crest, as illustrated in Fig. 12. In this study, all three weir crest shapes (i.e., sharp-crested, half round, and quarter round) experienced the three flow regimes (clinging, leaping, and springing). Sometimes the weir would experience a mixture of leaping and springing conditions simultaneously at different locations on the weir. The water would be springing near the upstream apex and gradually change to a leaping condition near the downstream apex.

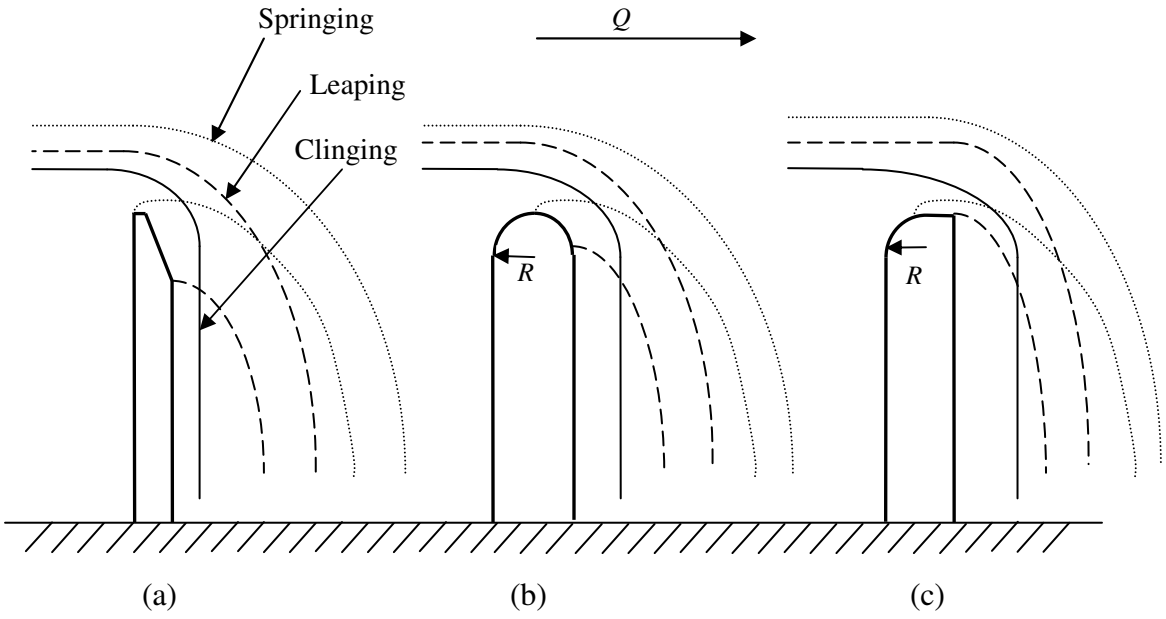

Figure 12. Three different flow regimes observed during testing for (a) sharp-crested, (b) half round, and (c) quarter round weirs.

Clinging flow only occurred for very low H_t/P. The taller weirs experienced clinging flow whereas the shorter weirs did not because H_t/P could not get low enough. According to Johnson [12], the depth of the tail water affects the negative pressure at the downstream edge of the weir for clinging flow. As the tail water level increases, the negative pressure becomes less negative and C_d decreases.

Leaping flow occurred when the flow momentum was sufficient for the water to separate from the downstream face of the weir. The locations of the leaping flow were different for each crest shapes. For the sharp-crested weir, the water would leap from the bottom of the chamfer on the downstream side of the weir. For the half round crest, the water would leap from the bottom of the round on the downstream side of the weir. For the quarter round crest the water would leap from the downstream edge of the flat portion of the crest. The leaping locations are shown in Fig. 13.

Springing flow occurred when the flow momentum was high enough to cause the water to spring from the separate from the crest flow boundary near the crest high point or even further upstream. The springing locations are also shown in Fig. 12. The water springs from the upstream edge of the sharp-crested weir. The water springs from the top of the round of the half round crest, having a rounded approach on the weir crest. For the quarter round crest, the water springs from the top of the round and is not affected by the flat part of the crest, in effect, making it the same as the half round crest. It was observed that the half round and quarter round crests performed similarly when springing nappe conditions existed. The 10° and 15° oblique weirs never experienced fully springing nappe conditions, but experienced mixed springing and leaping conditions as described previously.

Johnson [12] explained how the nappe condition affects C_d. He was able to compare C_d for the three conditions at the same H_t/P and found that C_d was highest for clinging flow, followed by leaping flow, and lowest for springing flow for the sharp-crested and broad crested weirs he tested. In the present study, it was not possible to have the three conditions for the same H_t/P; but it was found that when the flow conditions changed as H_t/P was varied, C_d would change drastically. It was very noticeable for the change in leaping to springing flow for the sharp-crested weirs.

Effective Length vs Centerline Length

The effective length L_e was used in calculations instead of the centerline L. This was done to remove the length of the weir that appears to pass little or no discharge and to facilitate a comparison between oblique weir data from the current study and the Tullis et al. [10] labyrinth weir data. Figure 13 shows that little to no flow passes over the length of the weir associated with the downstream apex. The same length of the weir

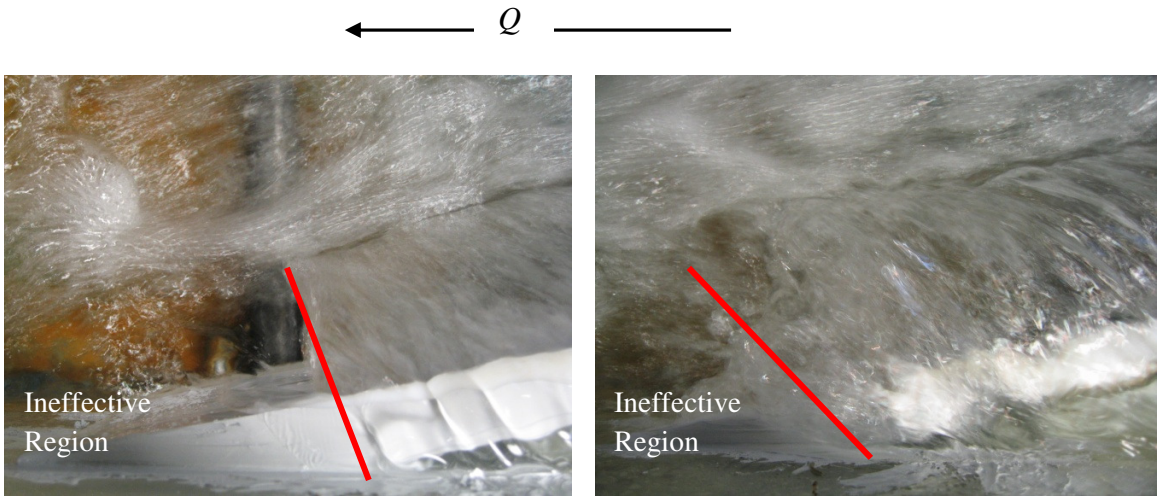

Figure 13. Flow over the downstream apex of the 10° sharp-crested weir with P = 12 inches and H_t/P = (a) 0.089 and (b) 0.297.

associated with the upstream apex is ineffective at passing discharge as well because the sidewall does not allow for the flow to pass over the weir at the crest-normal direction. Uijttewaal [8] explains that the velocity increases above the weir and results in a change of flow direction towards the crest-normal direction. The water flows over the weir in a crest-normal direction at low H_t/P. As H_t/P increases, the streamlines change to less than the crest-normal direction until H_t/P becomes high enough that the streamlines do not change at all but stay straight down the channel. The water stays on the weir longer and the crest shape, relative to the streamline travel path, is changed from a circular crest to an elliptical crest shape as shown in Fig. 14, which may cause shifts in data.

Velocity Head Compared to Total Head

To show the importance of the velocity head, the percentage of the velocity head to H_t was calculated. The velocity head was only 0.3-2.6% of H_t for the 12-inch weirs with $\alpha = 90°$, making the velocity head least important in those situations. The velocity

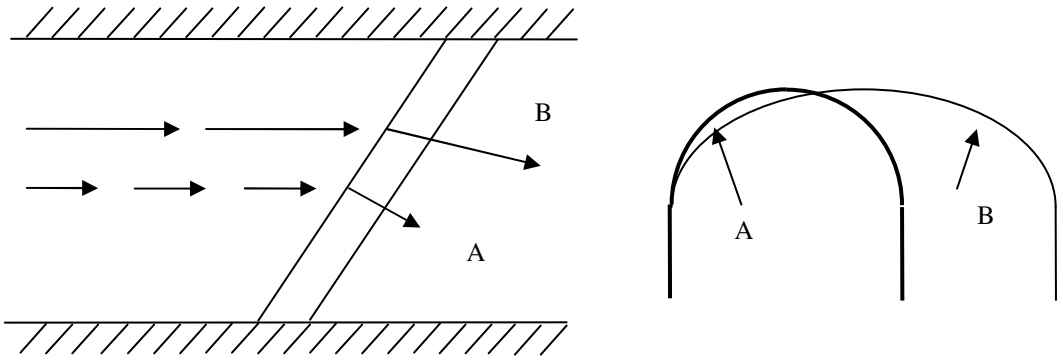

(a) (b)

Figure 14. (a) Streamlines change direction as H_t/P increases from A to B. (b) The crest shape changes from circular (A) to elliptic (B).

head was 23-29.3% of H_t for the 4-inch weirs with $\alpha = 10°$, making the velocity head most important in these situations. As expected the velocity head would become larger as Q increased. As α decreased, the velocity head became a larger part of H_t. As P decreased the velocity head also became a larger part of H_t.

Discharge Coefficients

C_d vs. H_t

Figures 15-17 show C_d data for the specific sharp-crested, half round, and quarter-round-crested weirs, respectively. The data for each of these figures are for vented nappe with leaping, springing, and mixed flow conditions. General observations are that C_d mostly decreases with increasing H_t, with the exceptions of the quarter round at low heads, and the sharp-crested normal weir ($\alpha = 90°$). As α increases and becomes closer to a normal weir, C_d normally increases. For each α, C_d increases as P increases, though the increase gets smaller as α gets closer to 90°.

The change from leaping to springing conditions for the sharp-crested weir can be seen in Fig. 14 at $H_t = 0.12$. The discharge coefficient drops from about 0.68 to about 0.60 for the 15° oblique sharp-crested weir with $P = 8$ inches. There is a similar drop for the same weir with $P = 12$ inches. The change from leaping to springing flow conditions for these weirs was very abrupt. The change for the half round and quarter round crests was not so abrupt. The nappe would start leaping from the positions shown in Fig. 12 at low heads and move gradually up the half round crest or away from the downstream edge of the quarter round crest to the top of the round for both crest shapes.

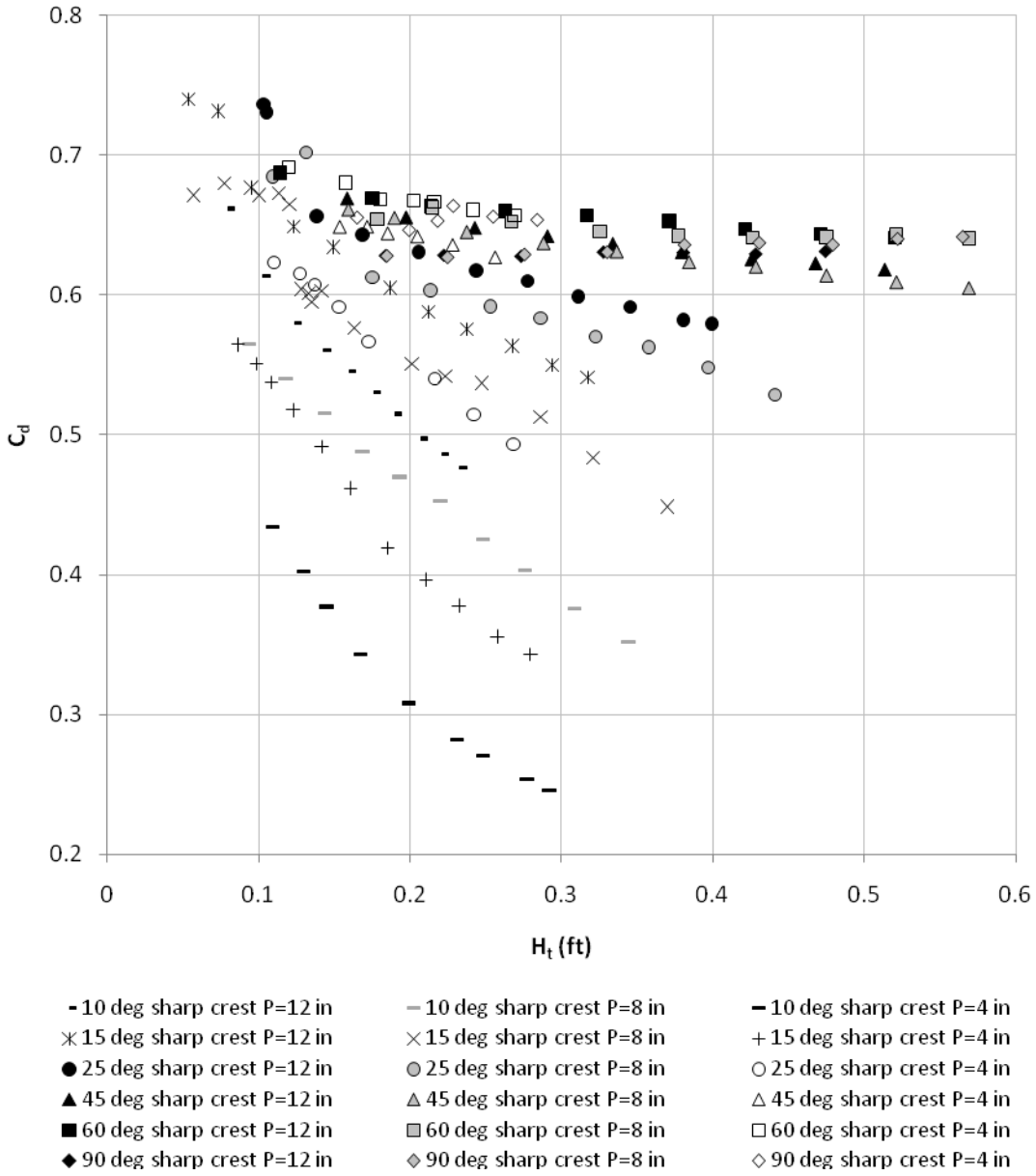

Figure 15. C_d vs H_t for vented sharp-crested weirs.

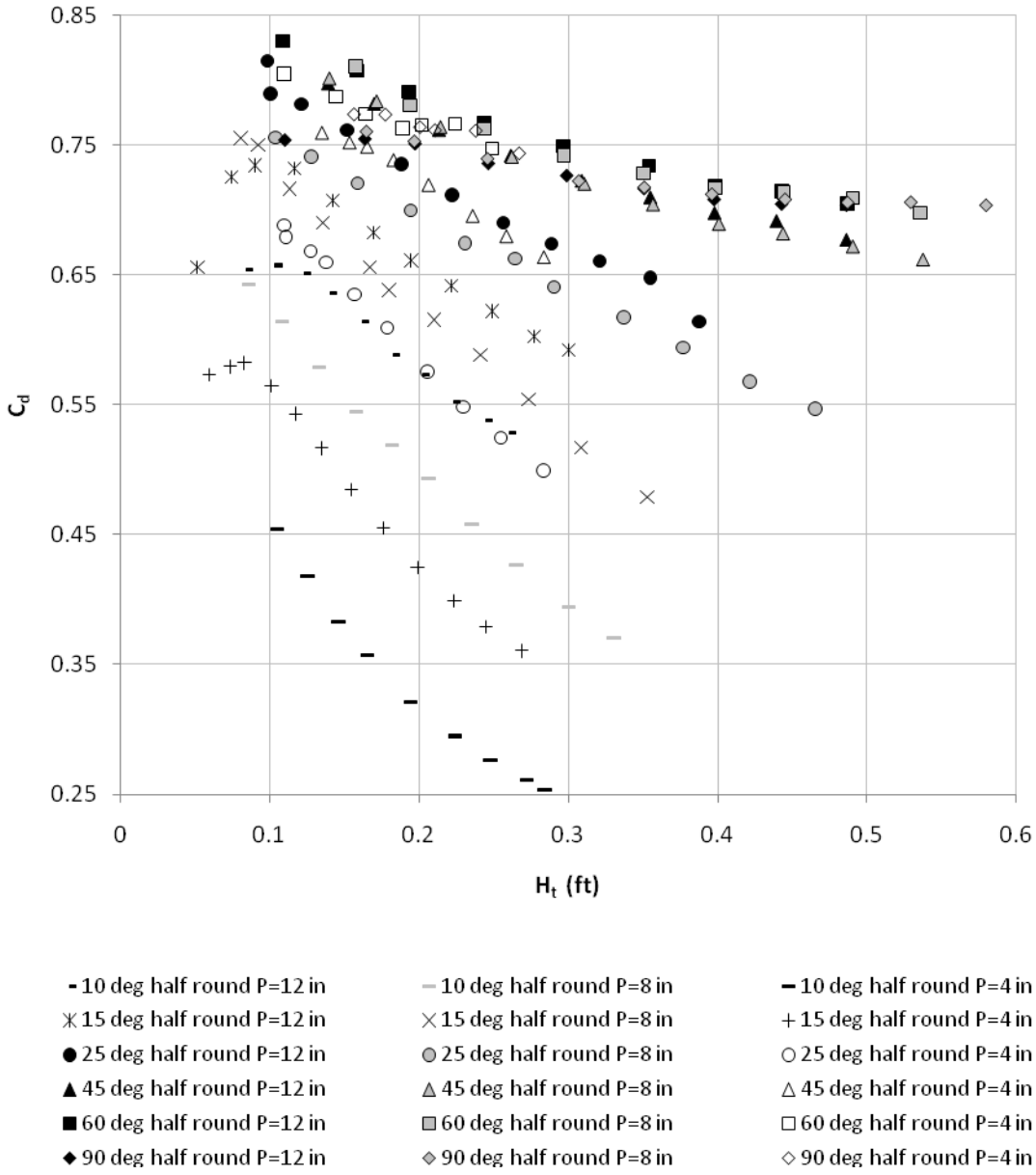

Figure 16. C_d vs H_t for vented half-round-crested weirs.

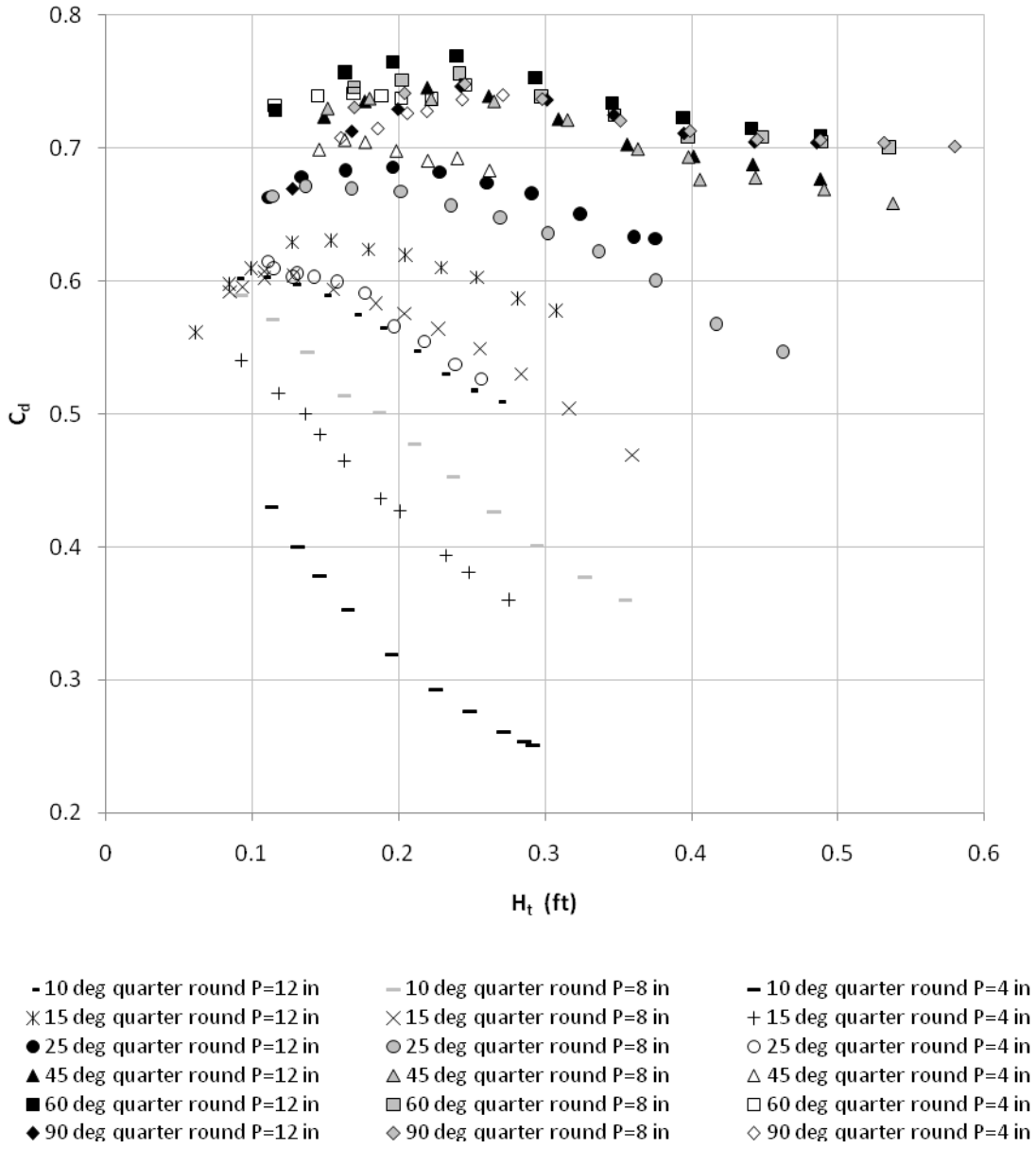

Figure 17. C_d vs H_t for vented quarter-round-crested weirs.

C_d vs. H_t/P

To make the data more useful in the design of weirs, C_d is usually plotted against the dimensionless parameter H_t/P. The weir height is an important parameter in weir design. By dividing H_t by P, the value of C_d may be for any weir as long as it has the same H_t/P value. This is also done to help collapse the family of curves for each α in Figs. 15-17 into a single efficiency curve. Figures 18-20 show C_d plotted against H_t/P for the vented sharp-crested, half round, and quarter-round-crested weirs, respectively. The lines drawn are for ease of distinction between different α.

A single smooth efficiency curve was developed for each α for the sharp-crested weirs. The 4-inch tall weirs for $\alpha \geq 25°$ featured higher C_d values than the other 8- and 12-inch tall weirs with the same α. There may be a couple of reasons for why this occurred. One reason is that there may be scale effects for such short weirs. Another reason may have to do with how the tail water affects the measurements. As shown in Fig. 21, the tail water is almost as high as the weir even at the lowest H_t possible. The tail water also created partial submergence that could have affected the weir discharge performance. Since the unit discharge downstream of the weir (in the weir vicinity)

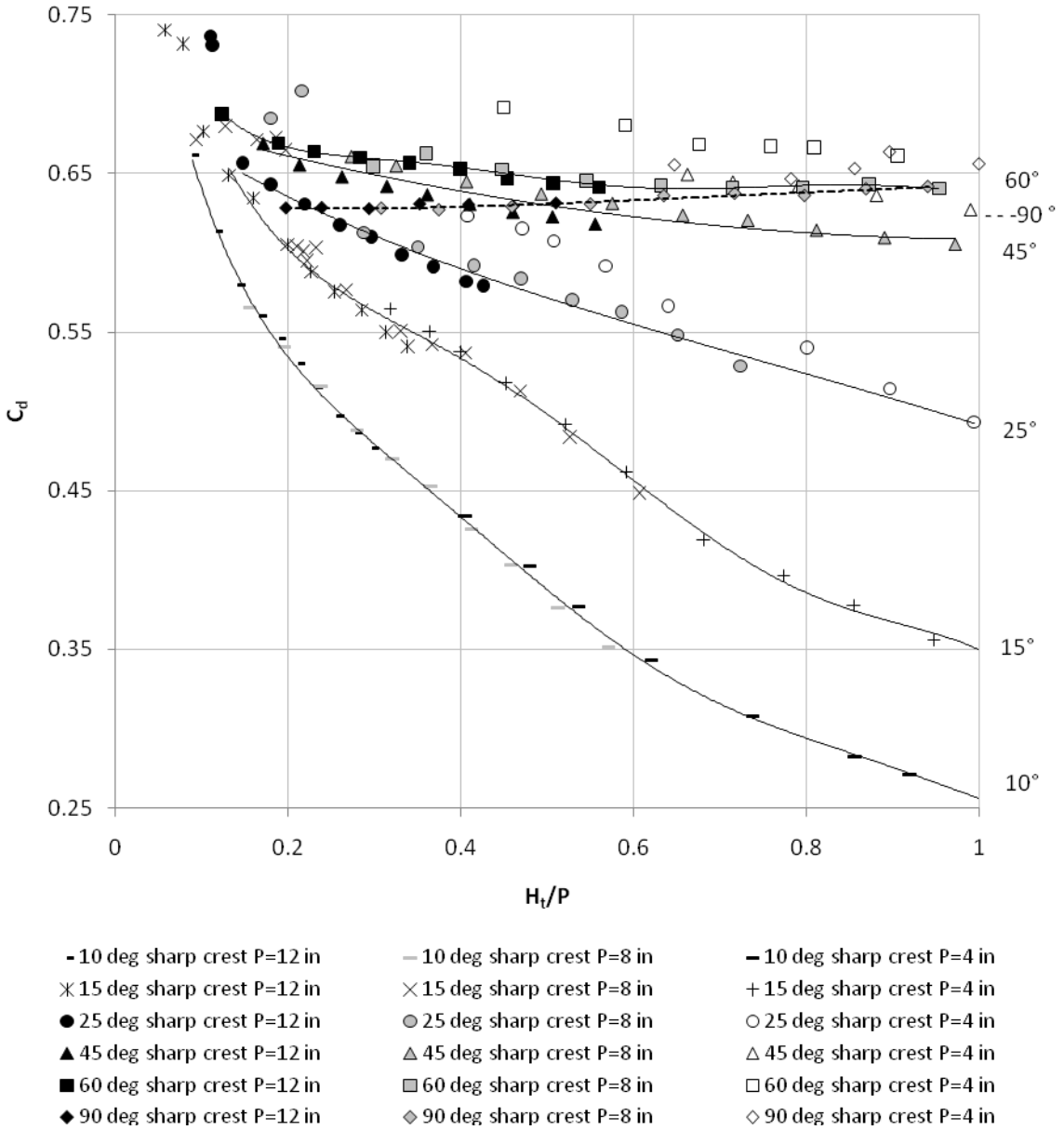

Figure 18. C_d vs H_t/P for vented sharp-crested weirs.

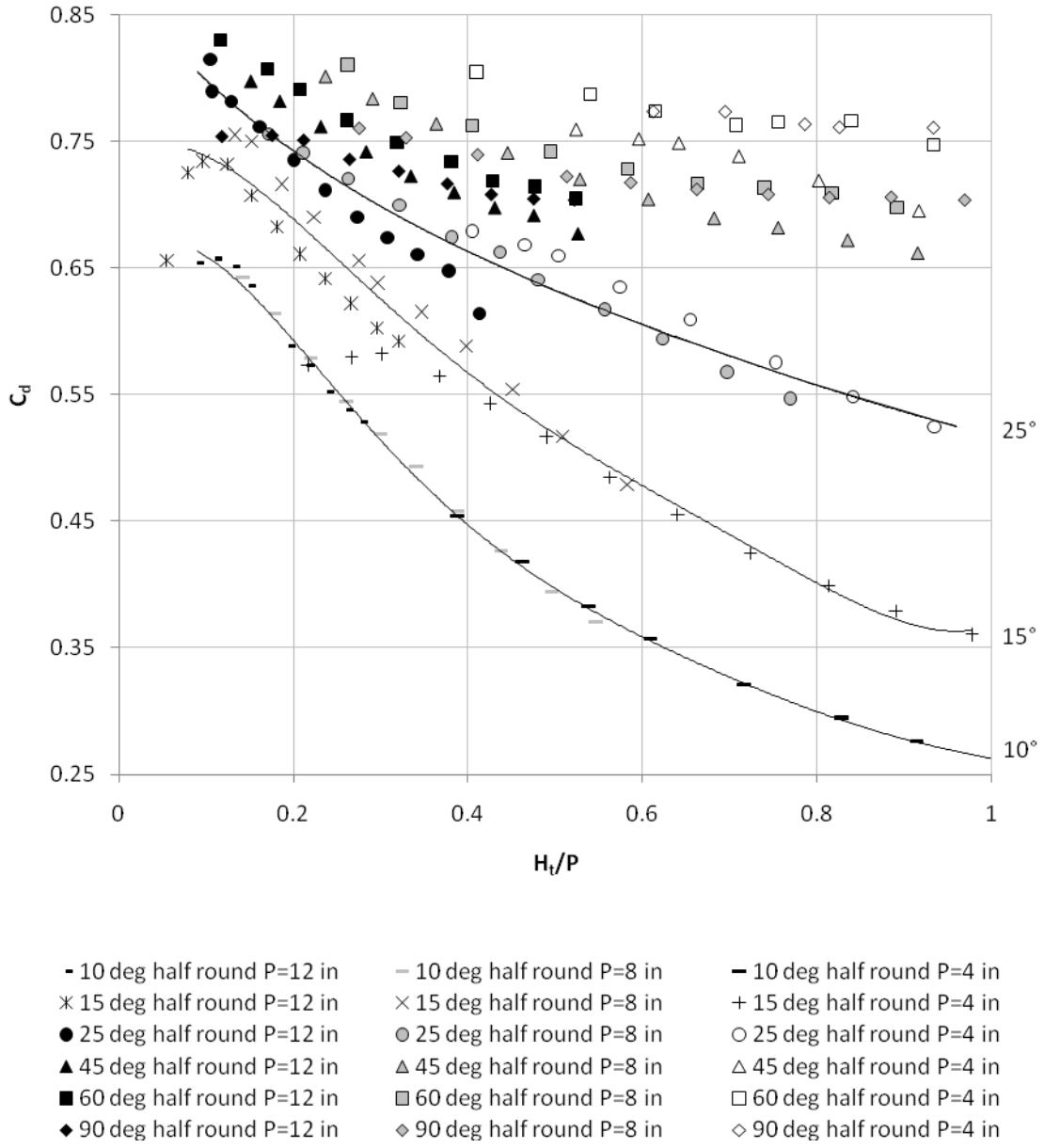

Figure 19. C_d vs H_t/P for vented half-round-crested weirs.

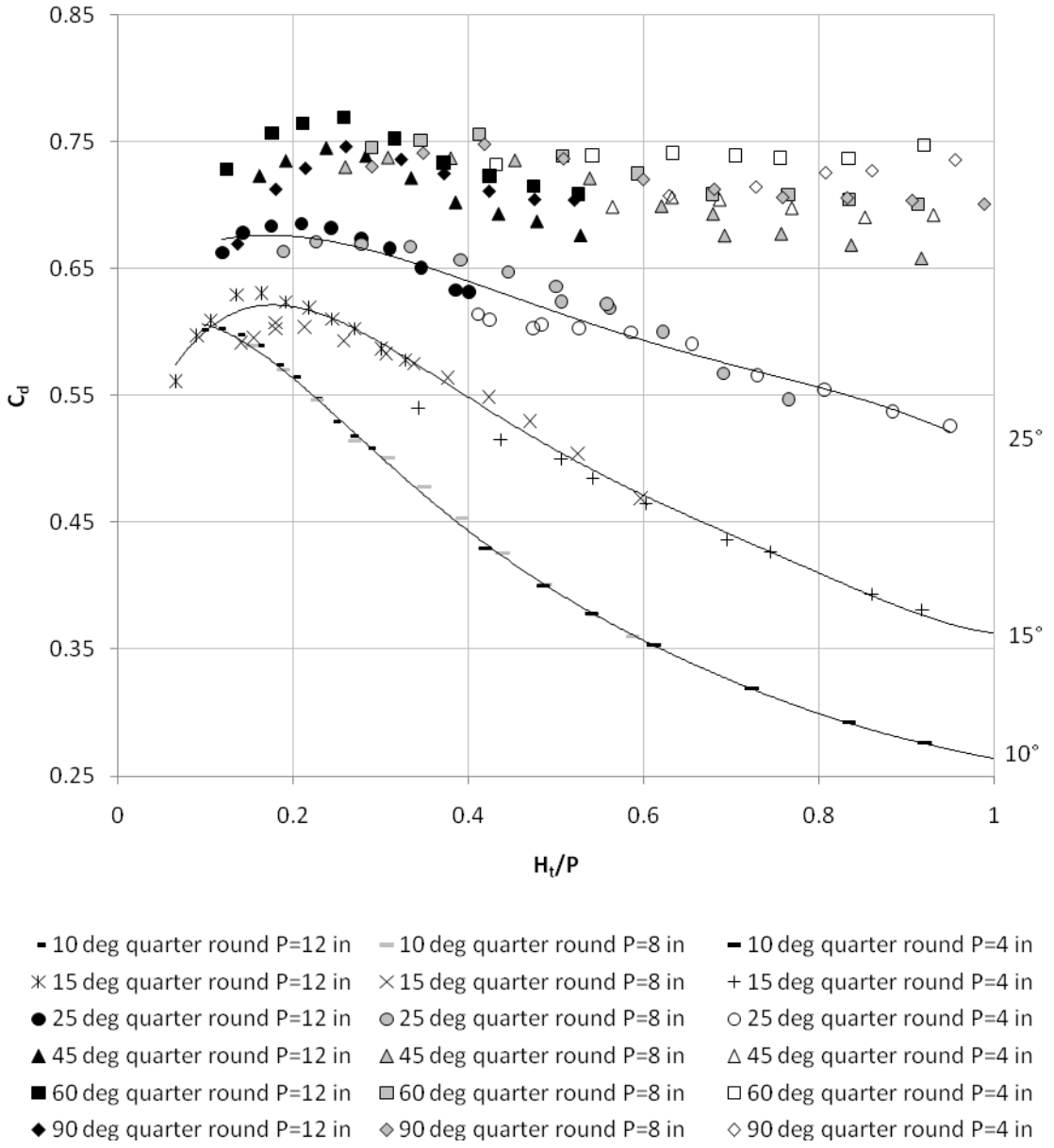

Figure 20. C_d vs H_t/P for vented quarter-round-crested weirs.

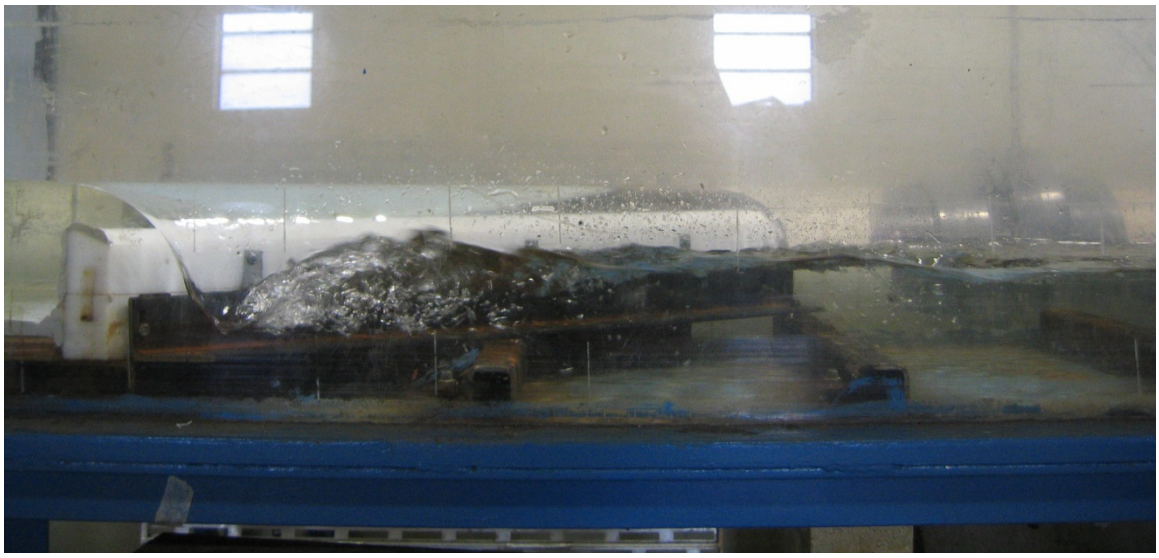

Figure 21. The tail water is almost as high as the weir for the lowest H_t possible for $P = 4$ inches, $\alpha = 45°$, non-vented sharp-crested weir.

increases in the direction of the flow direction, the flow depth also increases. As H_t/P increases, the downstream end of the weir begins to experience submerging tailwater depths before the upstream end, resulting in partial or segmental nappe aeration and influencing the discharge efficiency of the weir (i.e., smaller C_d values). Another feature that caused partial aeration was a localized hydraulic jump that developed just downstream of the upstream apex of the oblique weirs. The water level of the hydraulic jump was higher than the weir and would not allow for aeration at that point, while the rest of the nappe was aerated.

In Figs. 19 and 20, smooth curves could only be placed over the data for $\alpha = 10°$, 15°, and 25° for the half round and quarter-round-crested weirs. However, for $\alpha = 45°$, 60°, and 90°, no smooth curve can be generated for the half round and quarter-round-crested weirs. This is not unexpected as the data from Noori and Chilmeran [5] shown in Fig. 5 have shifts in the C_d values for weirs of different P with constant R. There may be

many reasons why the family of curves for these α does not collapse into a single smooth efficiency curve, including those given previously for the shift in the 4-inch tall oblique sharp-crested weirs.

One reason there are shifts may be that P is not the only important parameter affecting C_d. There may be other parameters such as the radius R of the crest, the thickness t of the weir, a combination of the two, or something else completely. More data needs to be taken to determine what parameters affect the half round and quarter-round-crested weirs.

The angle of the oblique weir may affect the streamlines because if α is small, the streamlines may stay closer to the crest-normal direction longer, which would explain why the smoothest efficiency curve is for $\alpha = 10°$ for both the half round and quarter-round-crested oblique weirs. The curves do not collapse as well for the 25° weirs and then not at all for higher angled weirs.

For designing oblique weirs with heights greater than 12 inches for α values that exhibit weir height-dependent C_d variations, the 12-inch tall half round and quarter-round-crested weir data are recommended since the tailwater and scale effects for the 12-inch tall weirs should be at a minimum, relative to the shorter weirs. Also, having a lower value for C_d (taller weir) would be more conservative for design. The 12 inch tall weir data may be extrapolated for a larger range of H_t/P, and other α may be interpolated.

Measurements were made for the non-aerated conditions when possible. Figures 22-24 show C_d for the non-aerated sharp crest, half round, and quarter-round-crested weirs, respectively. The discharge coefficients are higher than those for the vented weirs as expected. Non-aerated flow conditions could not be established for the 10° and 15°

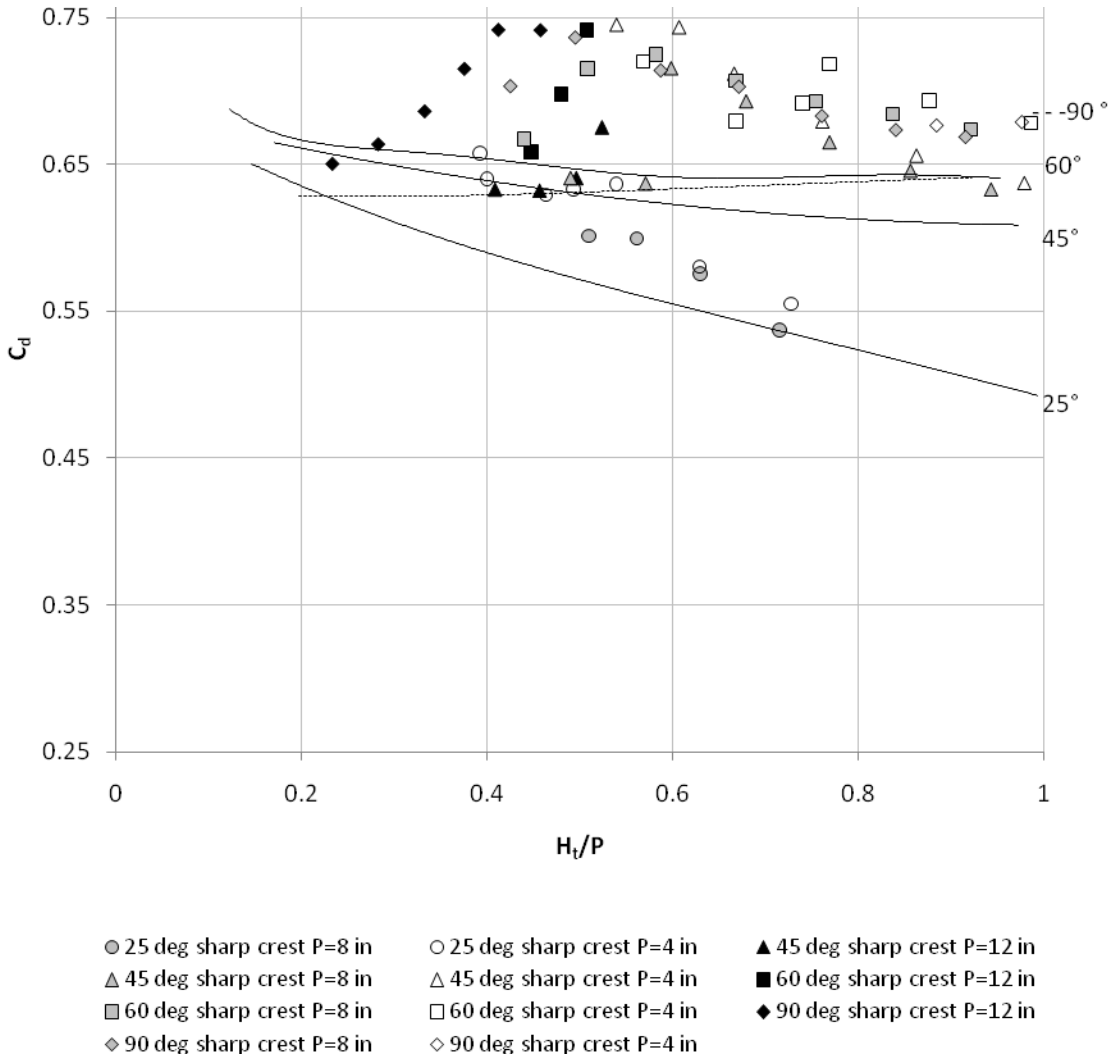

Figure 22. Non-vented data points for sharp-crested weirs.

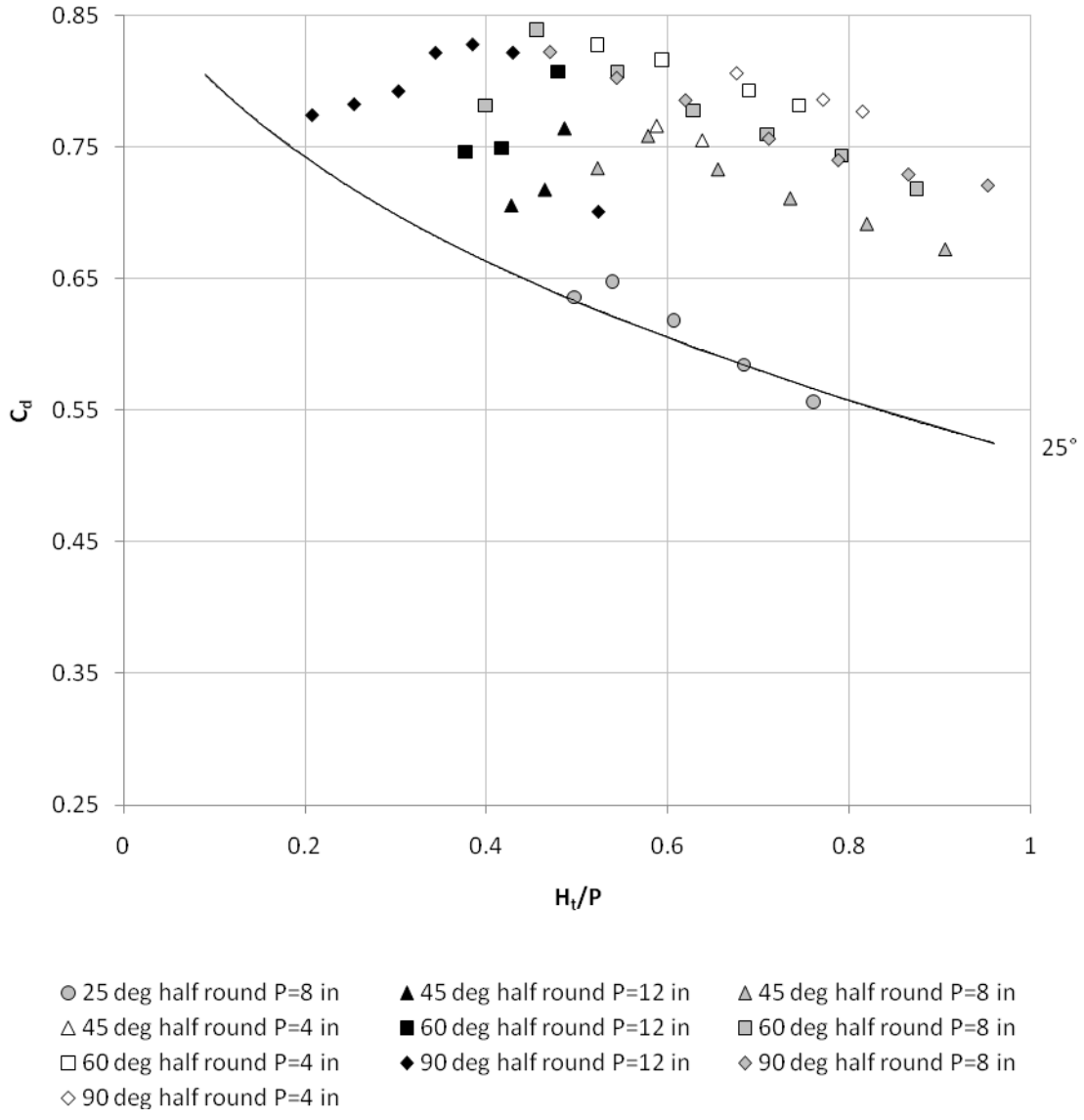

Figure 23. Non-vented data points for half-round-crested weirs.

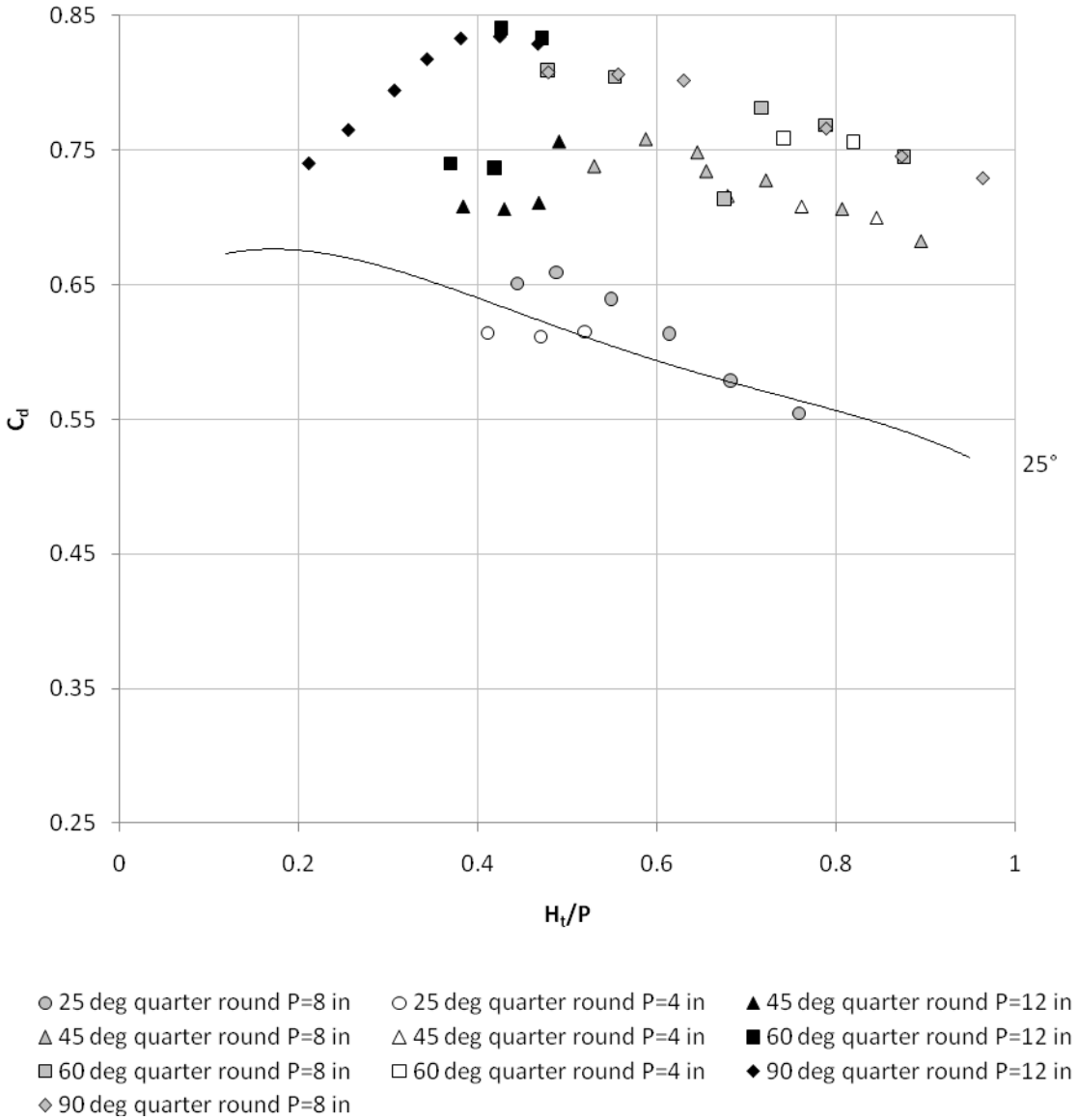

Figure 24. Non-vented data points for quarter-round-crested weirs.

oblique weirs due to the naturally occurring gaps that were present between the nappe and sidewall boundaries at the downstream apex. Only a few non-aerated data points were possible for the 25° oblique, but as α became larger, the range of non-aerated conditions increased. At low H_t/P, the differences between the vented and non-aerated data were small. The differences increased and then slightly decreased as H_t/P increased. As with the vented data, shifts can be observed in the non-aerated C_d data.

Comparison to Previous Studies

The vented oblique sharp-crested weir C_d data were compared to the data and Eq. (7) determined by Borghei et al. [3] in Fig. 25. The half round data were compared to the half round crest labyrinth weir data by Willmore [11] in Fig. 27. No comparison to the data of Noori and Chilmeran [5] or Eq. (13) was made. The data was determined for weirs that were not similar to those of the present study, making comparison impossible. Equation (13) could not be independently verified using the Noori and Chilmeran [5] data from which it was developed. Results from Eq. (13) did not match the data given by Noori and Chilmeran. The quarter-round-crested weir data were compared to the quarter-round-crested labyrinth weir data from Tullis et al. [10] in Fig. 29.

Sharp-crested Weirs

The discharge coefficients from the present study were converted from C_d to C_{dH}, where C_{dH} is based on H and L rather H_t and L_e to be consistent with the Borghei et al. [3] analysis. Figure 25 shows the comparison of calculated C_{dH} values from the present study with Borghei et al. [3] data and Eq. (7) for vented sharp-crested weirs. Figure 26

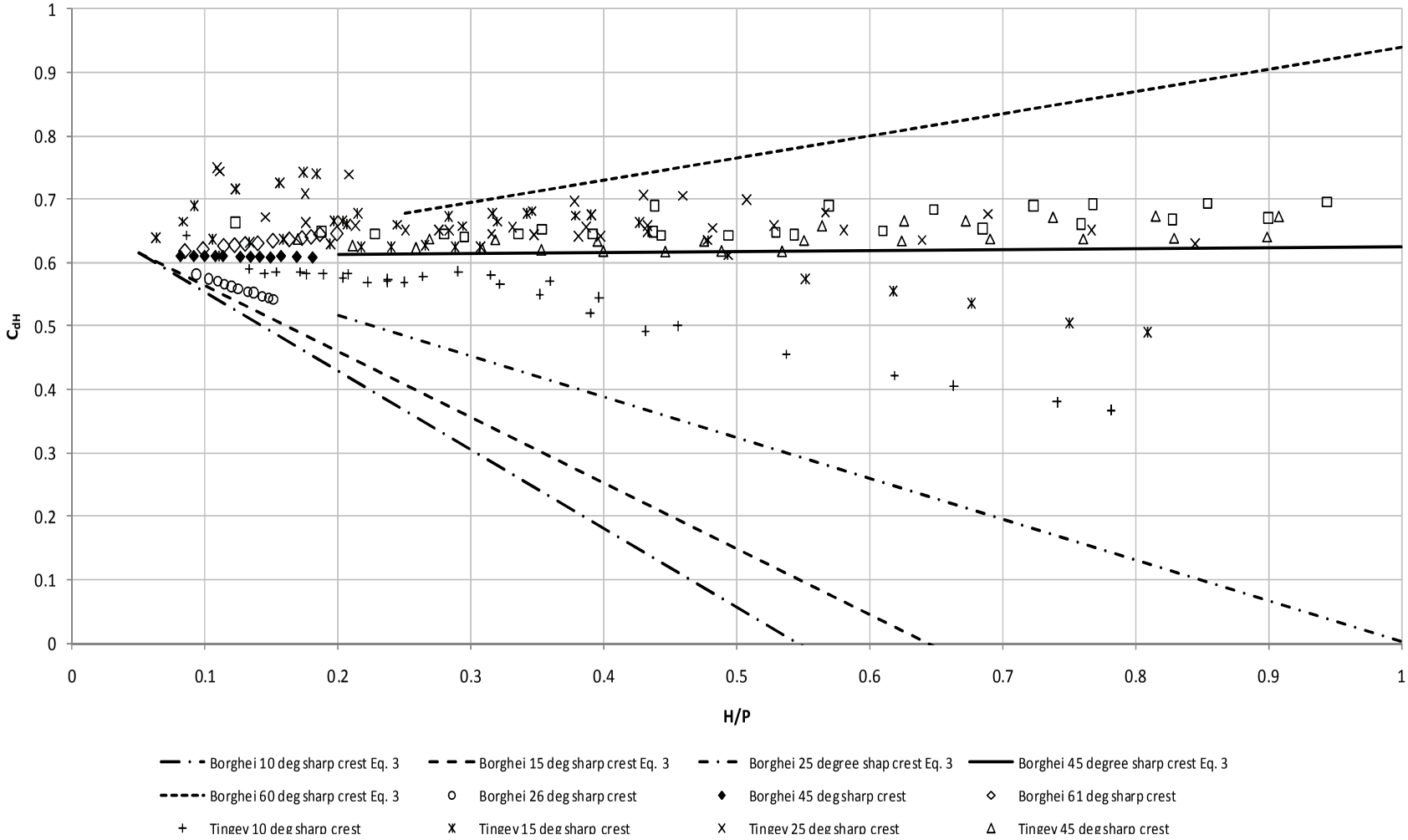

Figure 25. Comparison of calculated C_{dH} values from present study with Borghei et al. [3] data and Eq. (3) for vented sharp-crested weirs.

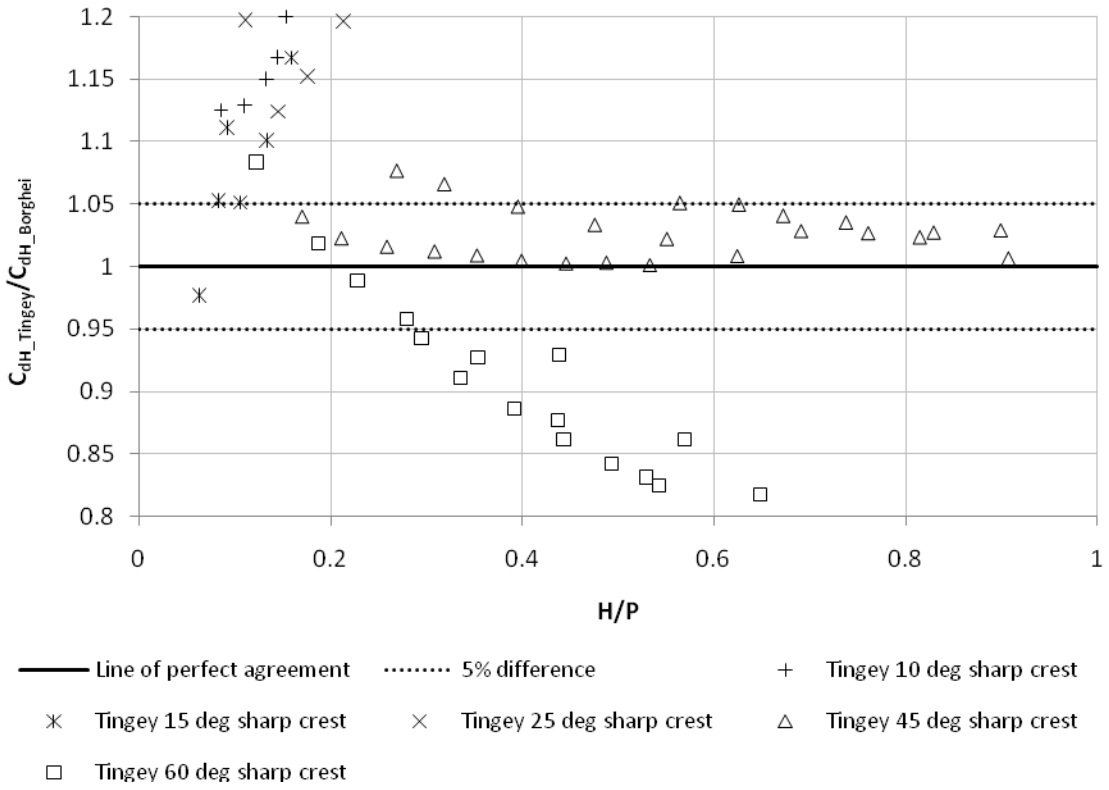

Figure 26. Agreement between calculated C_{dH} values from present study and Borghei et al. [3] for vented sharp-crested weirs.

shows the agreement between the two data sets. This was done by dividing C_{dH} from the present study by C_{dH} determined from Eq. (7). There seems to be little agreement between the data sets. The 45° oblique sharp-crested weir is the only one where the difference is less than 5%. The 15° and 60° oblique weirs begin within 5% difference, but quickly deviate. The 10° and 25° start with about a 12% difference and deviate rapidly as well. The rapid deviation from an agreement of 1.0 shows that Eq. (7) is indeed limited to low heads. The linear relationships given by Eq. (7) should not be used for oblique sharp-crested weirs with *H/P* greater than 0.2.

Half-round-crested Weirs

The C_d data from Willmore [11] was determined using L instead of L_e. His data was converted using L_e to make it comparable to the data from the present study. Figure 27 shows the comparison of calculated C_d values from present study with Willmore data for vented half round crest weirs. The agreement between data from the present study and Willmore is shown in Fig. 28. There appears to be fairly good agreement between the data. Most of the data agree to within 10% with a majority of those agreeing within 5%. The difference may arise due to the difference in the weir geometry. Willmore's weirs were trapezoidal labyrinth weirs. This gave his experimental set up an apex with a

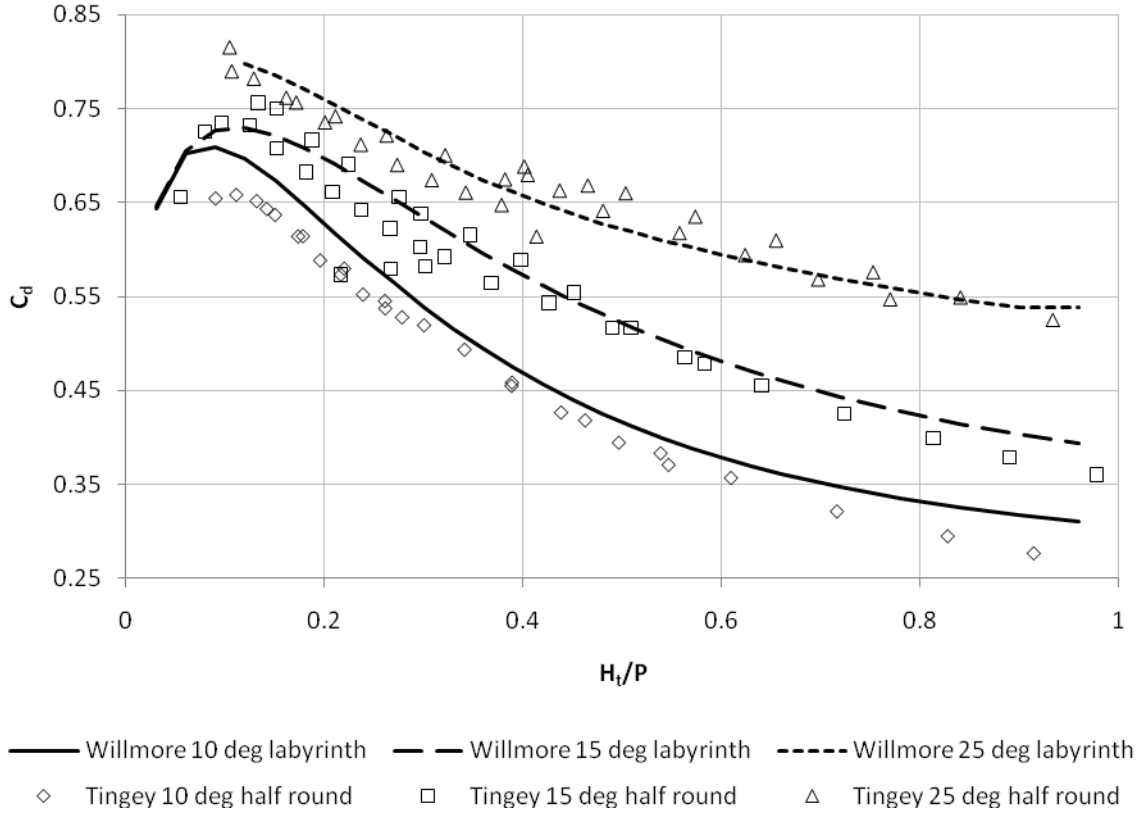

Figure 27. Comparison of calculated C_d values from present study with Willmore [11] data for vented half round crest weirs.

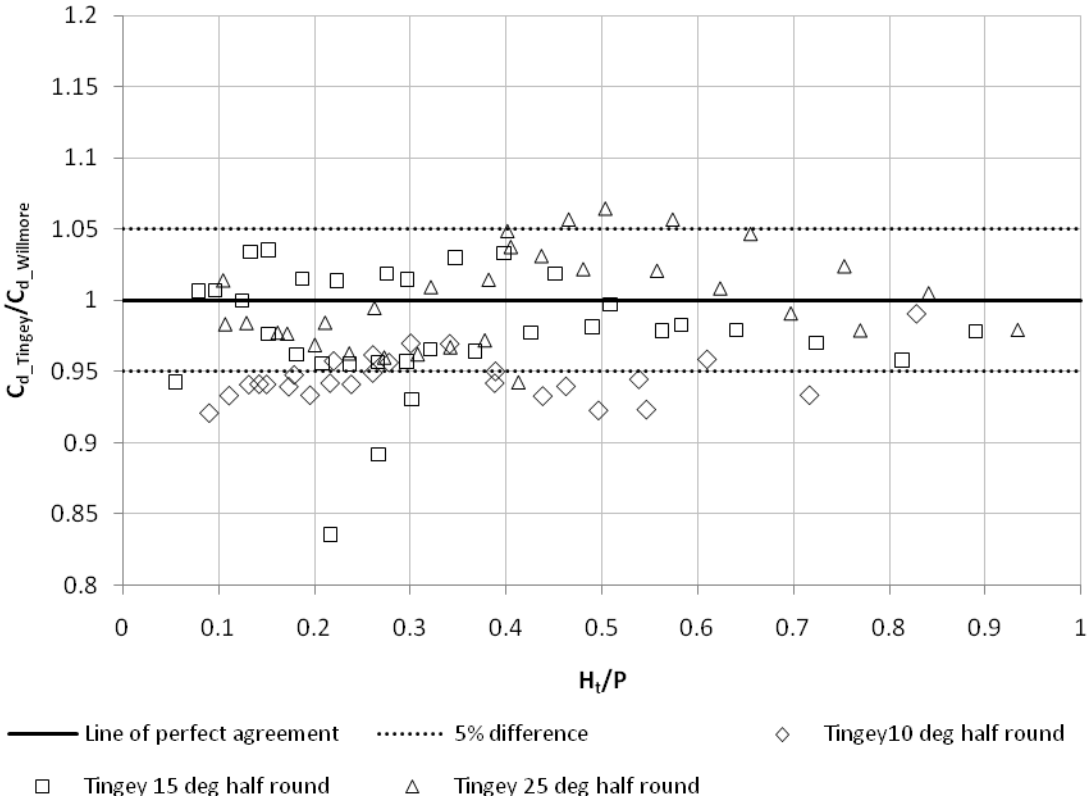

Figure 28. Agreement between calculated C_d values from present study and Willmore [11] for vented half round crest weirs.

weir section that was normal to the flow in the channel. The present study did not have any apexes in the set up. This difference in weir geometry could account for the difference in the results. It is the opinion of the author that, if there is a need, labyrinth weir data may be used in the design of half-round-crested oblique weirs with less than 10% error.

Quarter-round-crested Weirs

No conversion of the data from the present study or Tullis et al. [10] was performed as both used L_e and H_t to determine C_d. Figure 29 shows the comparison of

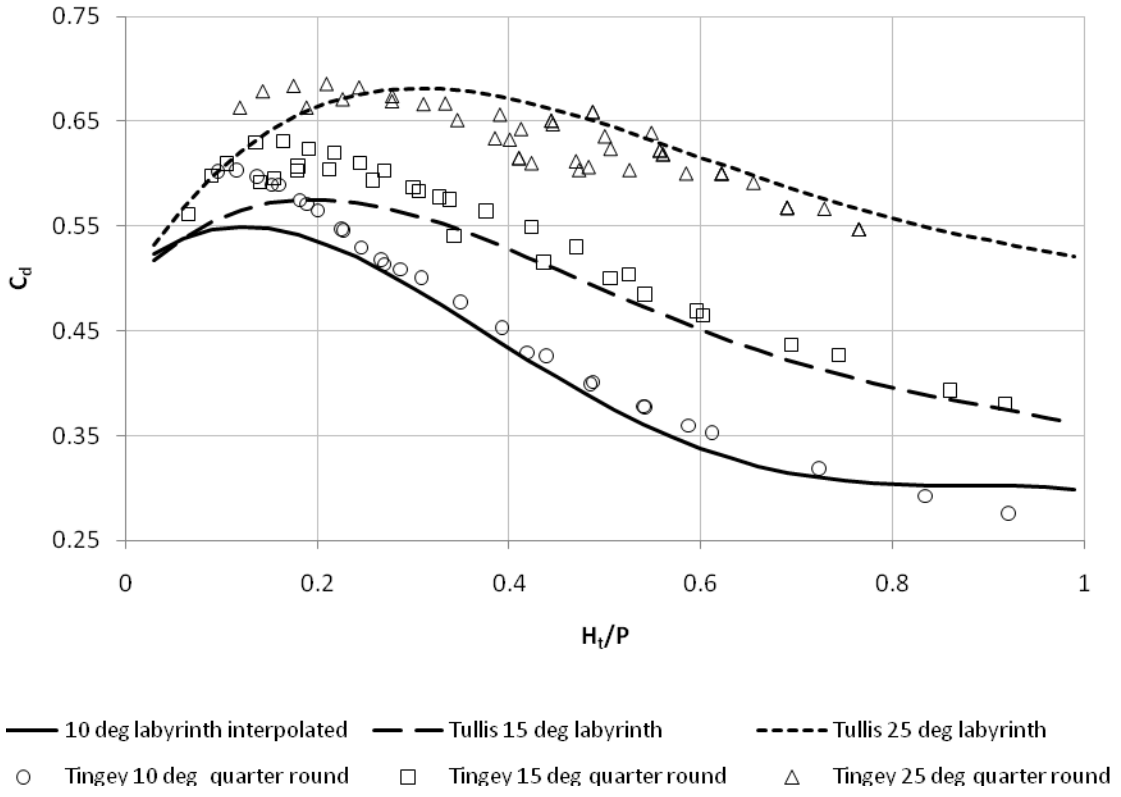

Figure 29. Comparison of calculated C_d values from present study with Tullis et al. [10] and Willmore [11] data for vented quarter round crest weirs.

calculated C_d values from present study with Tullis et al. [10] data for vented quarter round crest weirs. Data from Willmore [11] was used in interpolating the data for the 10° quarter-round-crested labyrinth weir. The agreement between the data is shown in Fig. 30. The data from the present study are higher than those from Tullis et al. [10] at H_t/P less than 0.2. They disagree between 5% to 10%. When H_t/P is greater than 0.2, most of the data agree to within 5%. Once again, the difference between the data may be attributed to geometry, as Tullis et al. [10] used trapezoidal quarter-round-crested labyrinth weirs. Again, it is the opinion of the author that, if needed, labyrinth weir data may be used in the design of quarter-round-crested oblique weirs with an error of less

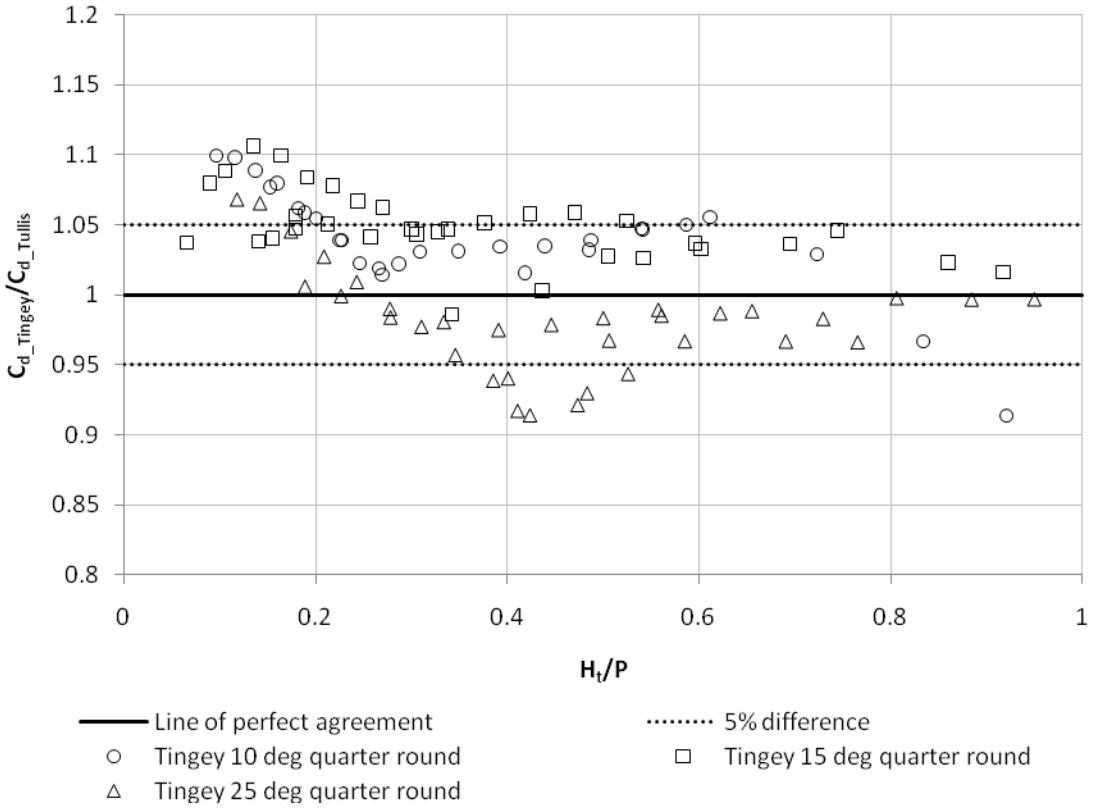

Figure 30. Agreement between calculated C_d values from present study and Tullis et al. [10] and Willmore [11] for vented quarter round crest weirs.

than 10%. The maximum error would occur when H_t/P is less than 0.2.

Effect of Oblique Angle and Crest Shape on Upstream Head

The purpose of this study was to learn more about the hydraulic characteristics of oblique weirs. This was done to help solve the problem that was described previously in the introduction, which is increasing flow through an open channel where there is limited freeboard when a diversion structure is needed. It was said that a weir with a longer length would increase flow without increasing the upstream head as much as a weir with a shorter length. It was also said that the crest shape could affect the upstream head.

Figure 31 shows how the crest shape and α affects H for the 12 inch tall weirs in the present study. The upstream head increases most rapidly for the normal sharp-crested weir. The upstream head increases the slowest for the 10° oblique half-round-crested weir. From the figure, it can be seen that as α decreases and the oblique weir becomes longer, the discharge capacity increases and more freeboard is available for flood routing, because H is not increasing as rapidly. This validates the hypothesis given earlier.

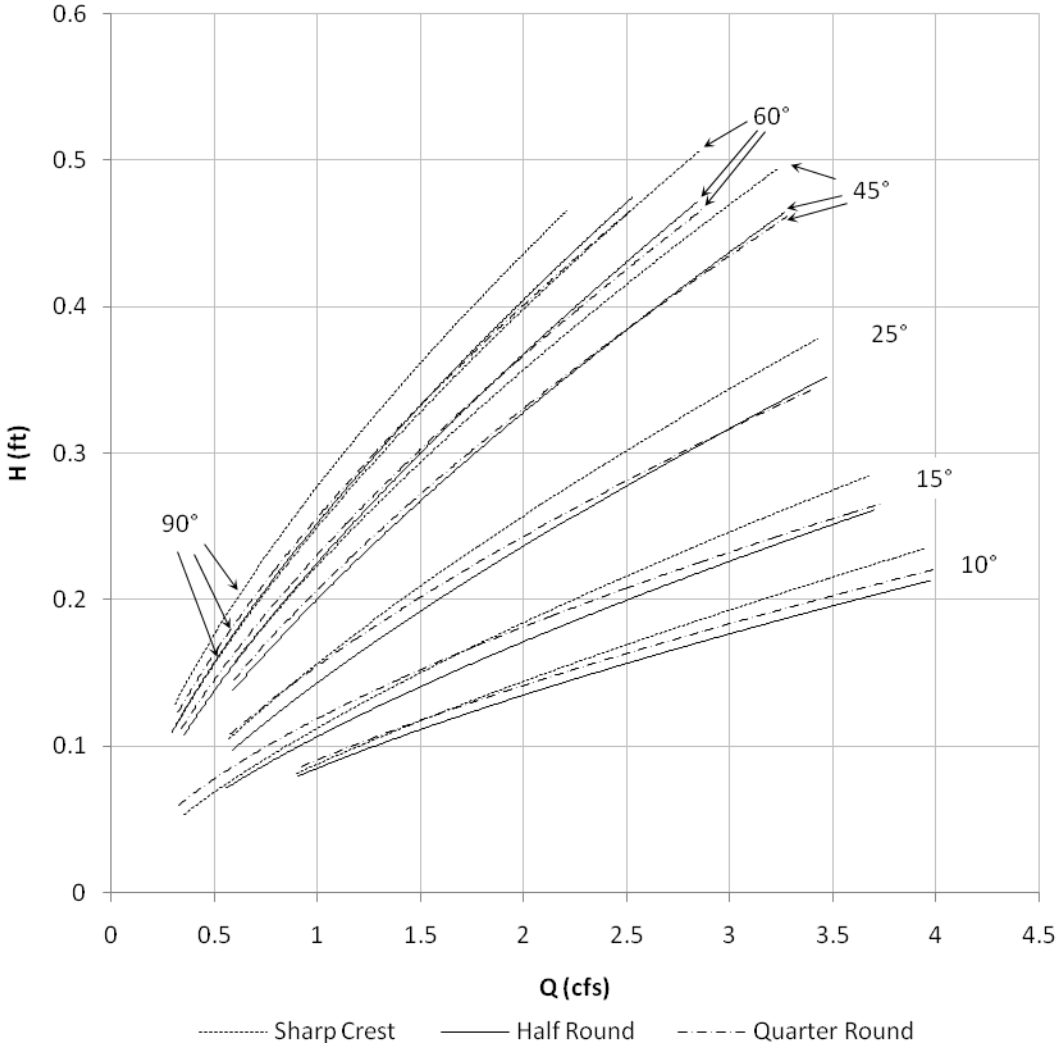

Figure 31. Comparison of how the different crests and angles affect H.
All weirs have P = 12 inch.

From Fig. 31 it can also be seen how the crest shape affects H. The half-round-crested weir is usually the most efficient, followed by the quarter-round-crested weir, followed by the sharp-crested weir which is the least efficient of the three crest shapes tested. The exception is the quarter-round-crested weir is less efficient than the sharp-crested weir for $\alpha = 15°$. It is not clear why this exception occurred. It can be seen in Fig. 31 where the quarter-round-crested weirs begin to act the same as the half-round-crested weirs due to the springing nappe condition. As α decreases, it takes more Q to reach the springing nappe condition for the quarter-round-crested weir. It also appears that there is more to be gained by changing the crest shape at higher angles than by changing the angle. For smaller angles, more is gained by decreasing the angle than by changing the crest shape.

SUMMARY AND CONCLUSIONS

The discharge coefficients were determined for 54 different weirs by measuring H_t for various Q for each weir. These weirs included sharp-crested, half round and quarter-round-crested weirs. There were 18 weirs for each crest shape with three weir heights for each angle tested. The oblique angles tested were 10°, 15°, 25°, 45°, 60°, and 90° with respect to the channel centerline, with the nominal weir heights being 4, 8, and 12 inches.

Different weir heights were tested to try to increase the range of H_t/P that was limited by the test facility. When the discharge coefficients were non-dimensionalized, it was found that for the sharp-crested weirs the family of curves could be collapsed into single curves for each α, but this was not the case for the half round and quarter-round-crested weirs. For these crest shapes, P is an important parameter that affects C_d.

The discharge coefficients for the vented aerated condition for each weir were compared to data from previous studies. The sharp-crested weirs were compared with the data and H-Q relationship from Borghei et al. [3], the half-round-crested weirs were compared with the labyrinth weir data from Willmore [11], and the quarter-round-crested weirs were compared to the labyrinth weir data from Tullis et al. [10]. It was found that the discharge coefficients for the sharp-crested weirs did not agree well except for the 45° oblique weir. This showed that the relationship determined by Borghei et al. [3] is limited to the range $H/P < 0.2$. The data from the other weirs agreed well and it was shown that oblique weirs could be considered as half cycle labyrinth weirs and data from

labyrinth weirs may be applicable to oblique weir design with a 10% maximum error possible

Finally, it was shown that increasing the length of a weir by placing it at an angle oblique to the centerline is an effective way to increase flow in a channel without sacrificing limited freeboard. Also, it was shown that the crest shape can help in overcoming the problem of needing to pass more flow without sacrificing freeboard.

REFERENCES

[1] Henderson, F. M., 1966, *Open Channel Flow*, Macmillan, New York, pp. 174-176.

[2] Aichel O.G. , 1953, "Discharge Ratios for Oblique Weirs," Z.VDI, **95**(1), pp. 26-27.

[3] Borghei, S.M., Vatannia Z., Ghodsian, and M., Jalili, M.R, 2003, "Oblique Rectangular Sharp-Crested Weir," Water and Maritime Engineering **156**, WM2, pp. 185-191.

[4] Borghei, S.M., Kabiri-Samani, A.R., and Nekoee, N., 2006, "Oblique Weir Equation Using Incomplete Self-Similarity," Canadian Journal of Civil Engineering, **33**, pp. 1241-1250.

[5] Noori, B.M.A., and Chilmeran, T.A.H., 2005, "Characteristics of Flow over Normal and Oblique Weirs with Semicircular Crests," Al_Rafidain Engineering, **13**(1), pp. 49-61.

[6] De Vries, M., 1959, "Oblique Weirs," Report WL, Delft Hydraulics, In Dutch.

[7] Wols, B., Uijttewaal, W., Labeur, R., and Stelling, G., 2006, "Rapidly Varying Flow over Oblique Weirs," *Proceedings of the 7th International Conference on Hydroscience and Engineering,* Philadelphia, PA, pp. 1-13.

[8] Uijttewaal, W.S.J., 2007, "Inundated Flood Plains and the Flow over Groynes and Oblique Weirs," Publs. Geophys. Pol. Acad. Sc., E-7 (401), pp. 245-254.

[9] Tuyen, N.B., 2006, "Flow over Oblique Weirs," MSc. Thesis, Delft University of Technology.

[10] Tullis, J.P., Nosratollah, A., and Waldron, D., 1995, "Design of Labyrinth Spillways," Journal of Hydraulic Engineering, **121**(3), pp. 247-255.

[11] Willmore, C., 2004, "Hydraulic Characteristics of Labyrinth Weirs," M.S. Report, Utah State University, Logan, UT.

[12] Johnson, M., 2000, "Discharge Coefficient Analysis for Flat-Topped and Sharp-Crested Weirs," Irrigation Science, **19**, pp. 133-137.